

CRUST 5.1: A global crustal model at $5^\circ \times 5^\circ$

Walter D. Mooney

U.S. Geological Survey, Menlo Park, California

Gabi Laske and T. Guy Masters

Institute for Geophysics and Planetary Physics, Scripps Institution of Oceanography
University of California, San Diego

Abstract. We present a new global model for the Earth's crust based on seismic refraction data published in the period 1948–1995 and a detailed compilation of ice and sediment thickness. An extensive compilation of seismic refraction measurements has been used to determine the crustal structure on continents and their margins. Oceanic crust is modeled with both a standard model for normal oceanic crust, and variants for nonstandard regions, such as oceanic plateaus. Our model (CRUST 5.1) consists of 2592 $5^\circ \times 5^\circ$ tiles in which the crust and uppermost mantle are described by eight layers: (1) ice, (2) water, (3) soft sediments, (4) hard sediments, (5) crystalline upper, (6) middle, (7) lower crust, and (8) uppermost mantle. Topography and bathymetry are adopted from a standard database (ETOPO-5). Compressional wave velocity in each layer is based on field measurements, and shear wave velocity and density are estimated using recently published empirical V_p - V_s and V_p -density relationships. The crustal model differs from previous models in that (1) the thickness and seismic/density structure of sedimentary basins is accounted for more completely, (2) the velocity structure of unmeasured regions is estimated using statistical averages that are based on a significantly larger database of crustal structure, (3) the compressional wave, shear wave, and density structure have been explicitly specified using newly available constraints from field and laboratory studies. Thus this global crustal model is based on substantially more data than previous models and differs from them in many important respects. A new map of the thickness of the Earth's crust is presented, and we illustrate the application of this model by using it to provide the crustal correction for surface wave phase velocity maps. Love waves at 40 s are dominantly sensitive to crustal structure, and there is a very close correspondence between observed phase velocities at this period and those predicted by CRUST 5.1. We find that the application of crustal corrections to long-period (167 s) Rayleigh waves significantly increases the variance in the phase velocity maps and strengthens the upper mantle velocity anomalies beneath stable continental regions. A simple calculation of crustal isostasy indicates significant lateral variations in upper mantle density. The model CRUST 5.1 provides a complete description of the physical properties of the Earth's crust at a scale of $5^\circ \times 5^\circ$ and can be used for a wide range of seismological and nonseismological problems.

1. Introduction

There are numerous applications for a global model of the seismic velocity and density structure of the Earth's crust and uppermost mantle. In the field of seismology, such a model provides regional travel times for locating earthquakes. Obviously, a good crustal model is the key ingredient to successfully monitoring regional-scale seismicity. Most mantle seismic tomographic methods use data sets which are quite sensitive to crustal structure but, at the same time, cannot resolve details within the crust. Hence accurate "crustal corrections" applied to these data sets are essential to improving the resolution of even large-scale mantle structure. Lateral variations in mantle density may also be inferred from long-wavelength gravity data if the density structure and thickness of the crust are reasonably well known. The crustal contribution to lithospheric stress

and crustal isostasy can be calculated from crustal thickness, density, and topography.

Previous global crustal models have provided various levels of detail. *Soller et al.* [1982] presented a crustal thickness map but did not specify seismic velocities or densities. *Hahn et al.* [1984] presented a model wherein the crustal structure was described in terms of irregularly shaped regions, each with a uniform structure. More recently, *Tanimoto* [1995] reviewed the crustal structure of the Earth using a wide range of seismic data, and *Nataf and Ricard* [1996] presented a model for the crust and upper mantle on a $2^\circ \times 2^\circ$ scale (3SMAC). This latter model was derived using both seismological data and nonseismological constraints such as chemical composition, heat flow, and hotspot distribution, from which estimates of seismic velocities and the density in each layer were made.

In this paper, we present a new global crustal model (CRUST 5.1) that is based on significantly more data than previous models. Compiling a new global crustal model is timely because of the availability of a large body of new data.

Copyright 1998 by the American Geophysical Union.

Paper number 97JB02122.
0148-0227/98/97JB-02122\$09.00

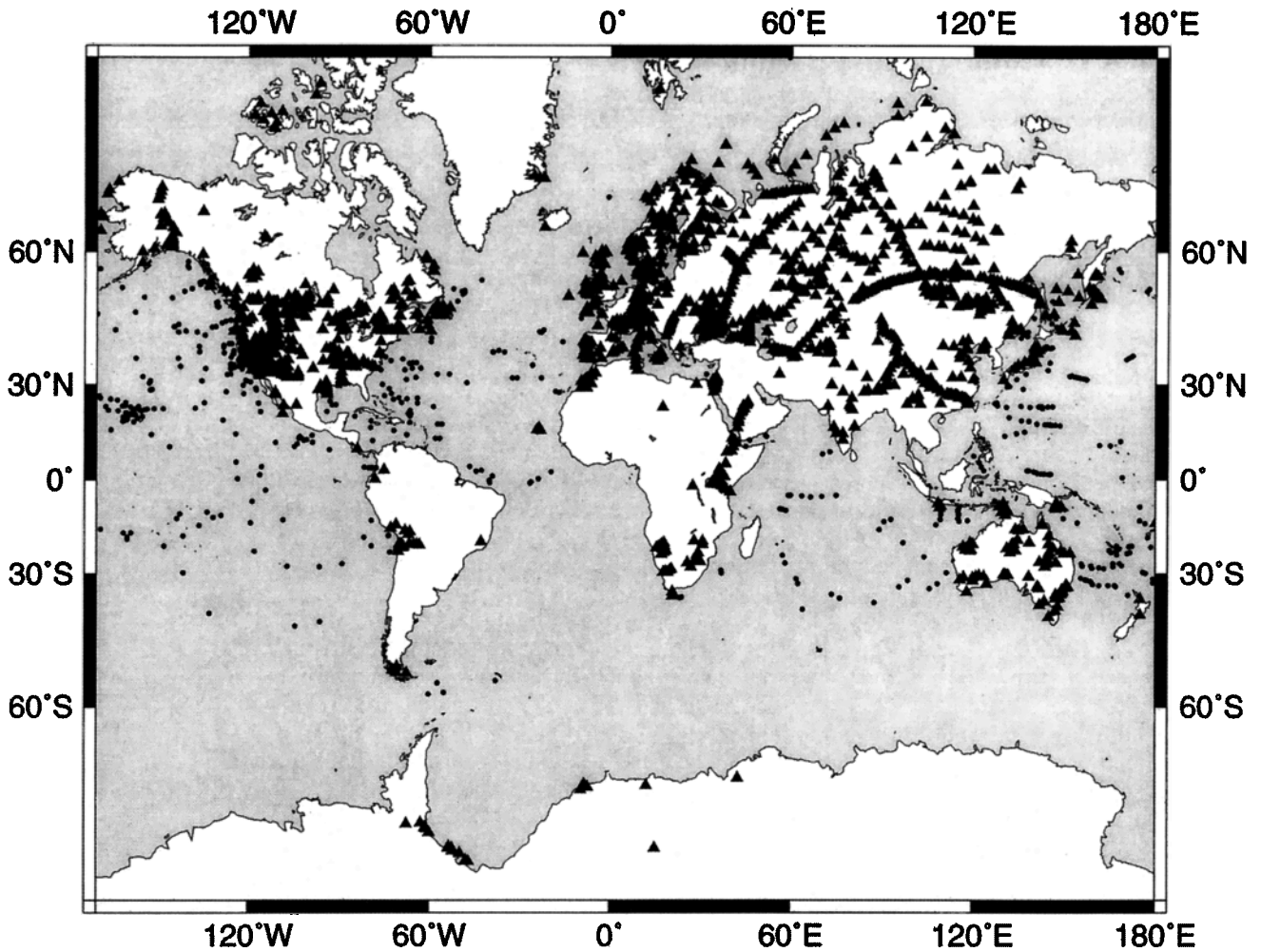


Figure 1. Location of seismic refraction profiles used in this study. Triangles correspond to locations within continents and on margins where a velocity-depth function has been extracted from a published crustal interpretation. These locations are generally at the midpoint between shot points along each profile. These data provide details on the compressional wave seismic velocity structure and, in about 10% of the cases, also the shear wave structure of the crust in a wide range of tectonic settings (Figure 2). Sources are cited by *Christensen and Mooney* [1995]. Solid circles are locations of oceanic refraction profiles [*Christensen, 1982*]. A standard crustal model is used for normal oceanic crust, and appropriate models are used for oceanic plateaus and other features (Figure 2 and text). Data selection and interpretation uncertainties are discussed in the text.

In the past several decades, many regions of the Earth have been explored by deep drilling and active seismic methods. These measurements, many of which have only recently been published, provide a wealth of information regarding the thickness and physical properties of sedimentary basins and the crustal structure of the ocean basins, margins, and continental interiors. Our new global model for the Earth's crust (CRUST 5.1) is based on an extensive compilation of information through the year 1995 (Figure 1). The inclusion of details regarding the thickness and physical properties of sedimentary basins is particularly important for many geophysical investigations since these basins are characterized by low densities and low seismic velocities and therefore have a significant influence on seismic wave propagation and the Earth's gravity field. Crustal structure has also been determined in many tectonically active regions such as mid-ocean ridges, oceanic plateaus, continental rifts, and orogenic belts. Published interpretations of the seismic velocity structure of the crust are now numerous enough and cover sufficiently diverse geological set-

tings that it is possible to calculate statistical averages for various geological settings such as Precambrian shields, extended continental crust, and passive margins. These statistical averages define a set of standard crustal sections (referred to here as crustal types). For the vast continental regions where, as yet, no seismic measurements are available, such as large portions of Africa, South America, and Greenland, we predict the crustal structure using the standard crustal types and present the statistical basis for these predictions.

We compare global maps of surface wave phase velocities predicted by our model with observations. The predictions of our model are strongly anticorrelated with the observations at long periods (i.e., larger than 80 s). There is much closer agreement between observed and predicted Love waves at a period of 40 s. Love waves at this period are quite sensitive to the shear wave velocity structure in the upper 60 km, a depth range that emphasizes the effect of the continental crust. We also compare the effect of our model to that of a commonly used previous model which is based on the crustal thickness

compilation of *Soller et al.* [1982] and find some significant differences. Our global crustal model can be used for a wide range of geophysical calculations of Earth structure. We illustrate this with a simple calculation of crustal isostasy that shows good agreement between predicted and real topography, the difference (residual topography) mainly being due to lateral density variations in the uppermost mantle.

2. Global Crustal Model

Our purpose is to create a model for the seismic velocity (V_p and V_s) and density structure of the crust and uppermost mantle that is at a large enough scale to be commensurate with the (nonuniform) global distribution of seismic field observations but that is also at a small enough scale to resolve significant lateral variations in crustal properties. In order to meet these competing goals, we have constructed our model using 5° × 5° tiles that measure 550 km by 550 km at the equator. In each tile, crustal properties are described by seven layers: (1) ice, (2) water, (3) soft sediments, (4) hard sediments, (5) crystalline upper, (6) middle, and (7) lower crust. An eighth layer is included to describe the elastic properties and density immediately below the Moho since this information is readily obtained from the seismic refraction profiles compiled here. Topography and bathymetry are provided as a separate file. Compressional wave velocity in each layer is based on field measurements, and shear wave velocity and density are estimated using empirical V_p - V_s and V_p -density relationships, as discussed below.

Since there are 2592 tiles in our 5° × 5° model and more than 2000 available field measurements of oceanic and continental crustal structure, a reasonable approach is to generalize the field measurements into a limited number of primary crustal types. This not only avoids having hundreds of different crustal models but also provides a basis for extrapolating measured crustal structure into regions lacking seismic refraction data. The use of primary crustal types is supported by the finding that there is a systematic variation of continental crustal structure as a function of basement age and tectonic setting [*Prodehl*, 1984; *Meissner*, 1986; *Holbrook et al.*, 1992; *Mooney and Meissner*, 1992; *Durrheim and Mooney*, 1994; *Christensen and Mooney*, 1995; *Pavlenkova*, 1996] and that oceanic crustal structure is remarkably uniform [*Orcutt*, 1987; *White et al.*, 1992]. Geological and geochronological information [e.g., *Goodwin*, 1991; *Exxon Production Research Company*, 1985] has been used to define geologic setting and basement age. From this information the primary crustal types were determined; 14 such types are shown in Figure 2. The Precambrian shields were divided into three age groups: Archean, Early-Middle Proterozoic, and Late Proterozoic. Precambrian platforms are a separate crustal type because of the highly variable thickness of sediments. Phanerozoic crust was divided into tectonic setting (extended crust, orogen, forearc, continental arc, etc.). Continental shelves, oceanic plateaus, and ocean-continent transitions are primary crustal types. The crustal structure used for the ocean basins is a simple four-layer approximation of published average crustal models [*Christensen and Salisbury*, 1975; *Spudich and Orcutt*, 1980; *White et al.*, 1992]. This structure includes layer 1 (sediments), layer 2 (pillow lava and sheeted dikes), and layer 3 (gabbroic layer). Oceanic layer 3 was subdivided into two layers in our model to conform to the three-layer description of continental crystalline crust. Thick oceanic crust, such as occurs above

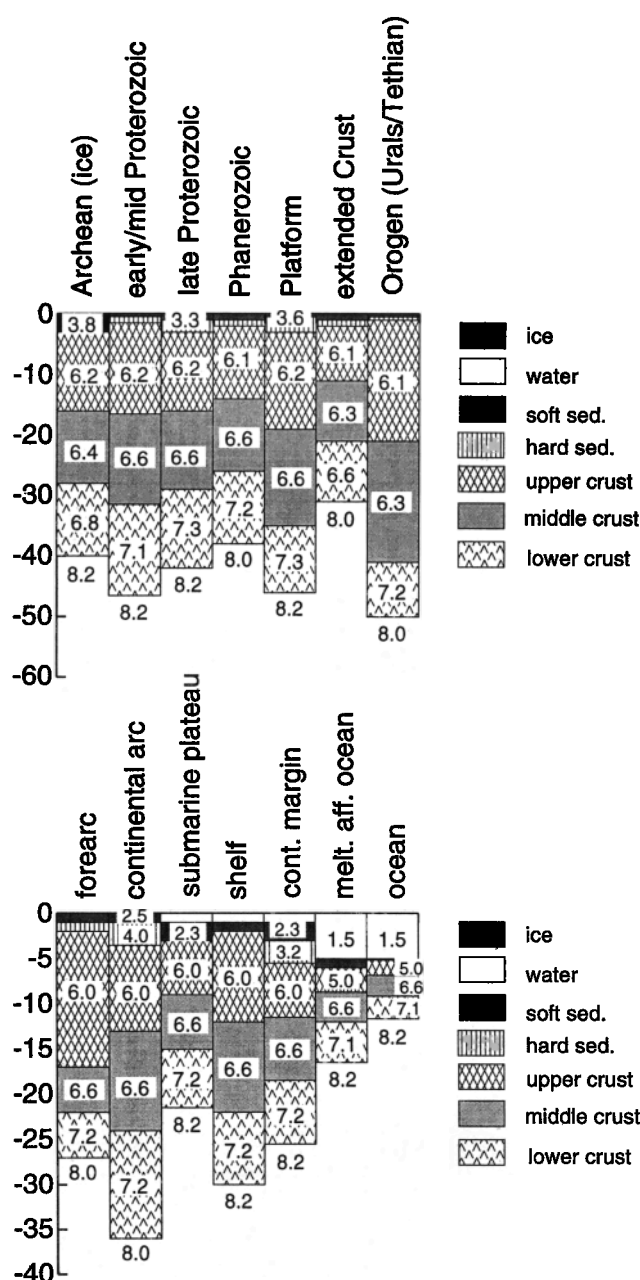


Figure 2. Primary crustal types used to construct the global crustal model CRUST 5.1. Each crustal type has seven crustal layers. The crustal layers are ice, water, soft sediments, hard sediments, and the upper, middle, and lower crystalline crust. V_p , V_s , and density are specified in each layer (only V_p is shown here). Values for the upper mantle below the Moho are also given. Each primary crustal type was derived by calculating an average model based on seismic refraction profiles recorded in crust of specific age or tectonic setting (see Figure 3 and text for details). There are many variants of each primary crustal type (not shown) to account for variations in ice and sediment thickness and to ensure close agreement with field measurements. A total of 139 different crustal models were needed to construct the global model CRUST 5.1. Melt affinity oceanic (melt. aff. ocean) crust occurs above mantle plumes, such as Hawaii.

hotspots, is assigned a separate crustal type. On continents, the average crustal structure for each primary type was statistically determined (Figure 3) from the field measurements indicated on Figure 1.

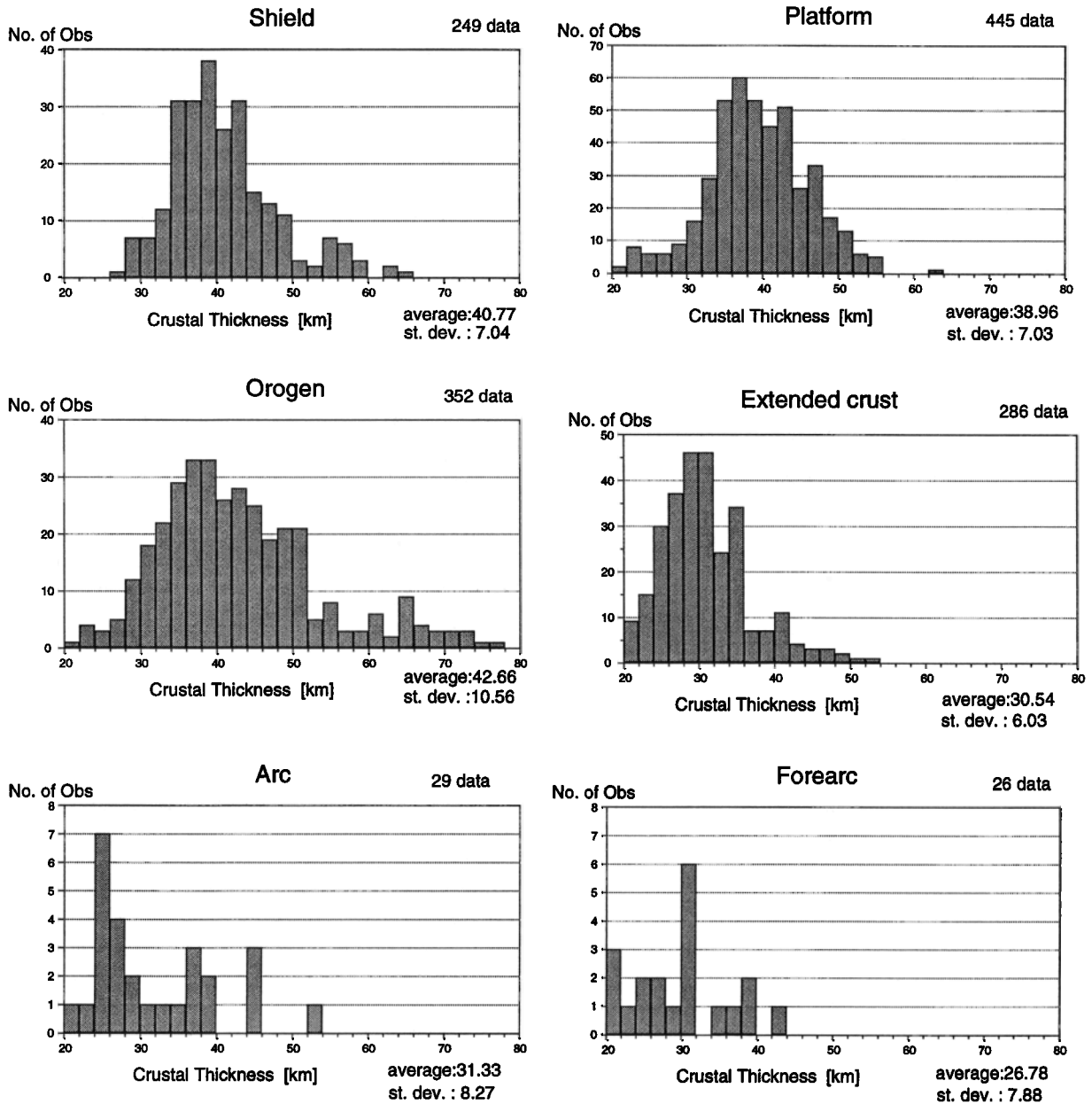


Figure 3a. Histograms of crustal thickness for six continental tectonic provinces from the individual point measurements (triangles) of Fig. 1. Average and standard deviation are indicated.

A primary crustal type was then assigned to each of the 2592 tiles, based on the geologic setting and (for continents) average basement age, thereby yielding a first-order global model. A much improved model could be made by allowing variants to the 14 primary types because many tiles do not fall entirely within one type. Typical examples include mixtures of the shields and continental margins, or orogens and adjacent platforms. In these cases a weighted average based on area was used, resulting in a crustal type whose seismic properties are intermediate between the two primary crustal types. Since we have also compiled detailed information on the global thickness of ice and sediments (see below), additional crustal variants were needed to satisfy these constraints while still honoring the statistically average structure of the crystalline crust. The use of crustal variants also ensured that the crustal model for those tiles with seismic refraction control matched the

measured velocities and crustal thickness. The final model (Plate 1) consists of 84 continental, 26 oceanic, and 23 shelf and transitional crustal models. An additional six unique crustal types were introduced for portions of the Red Sea, the Black Sea, and the Caspian Depression. The following sections describe the data sources and physical properties of the individual layers in the model.

3. Ice and Water Layers

In order to make as complete a model as possible, it was necessary to include ice as the first layer in our model. A thick layer of ice covers portions of the polar regions, particularly Antarctica and Greenland, where accumulations locally exceed 4 km (Plate 1b). The thickness of the ice in Antarctica was taken from the atlas of *Drewry* [1983], and in Greenland it is

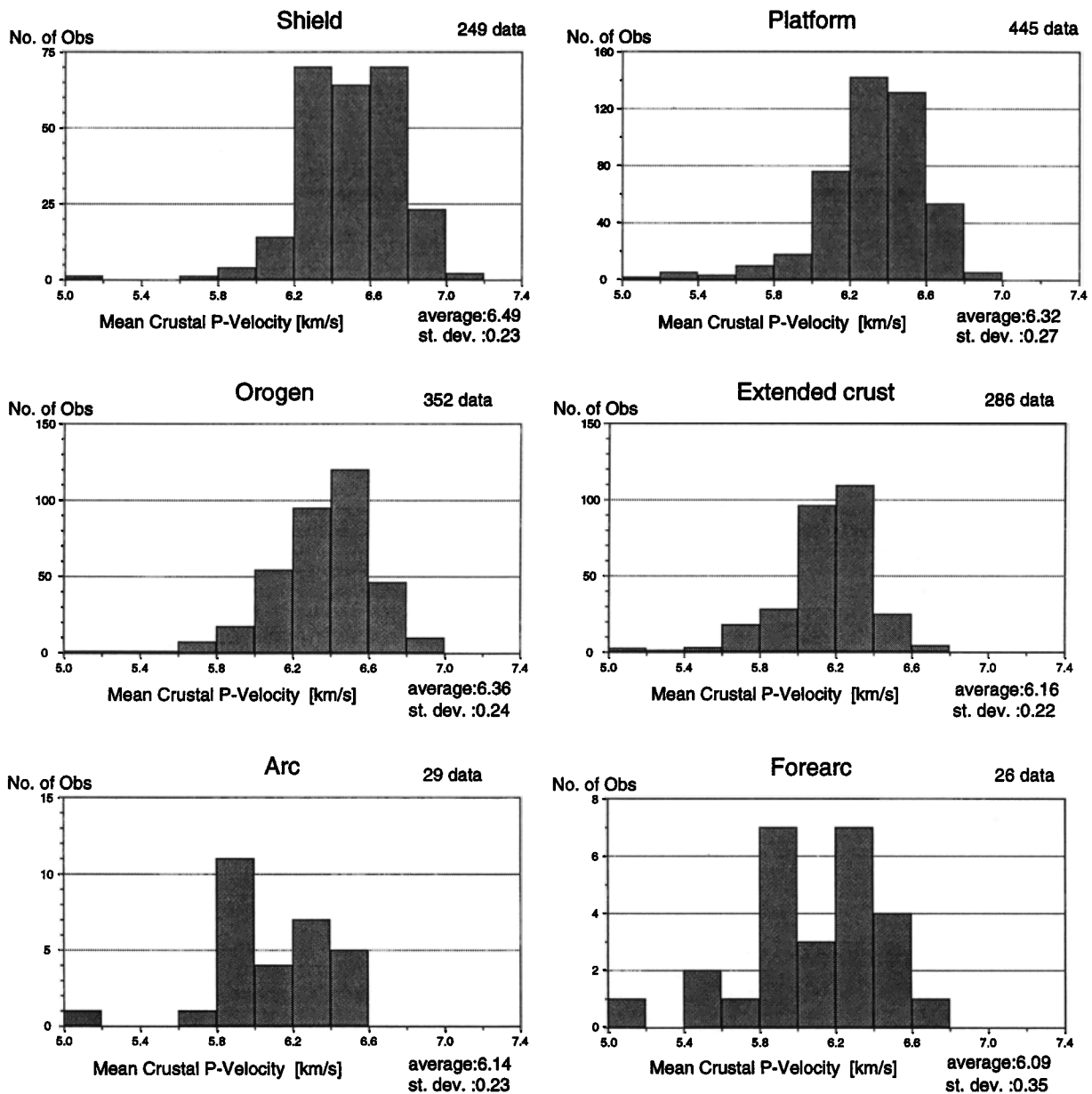


Figure 3b. Histograms of mean crustal velocity of the same six provinces as in Figure 3a. These and additional statistics for other tectonic provinces were used to construct the 14 primary crustal types (see text).

from Weidick *et al.* [1992]. Mean water depth (bathymetry) and topography within the $5^\circ \times 5^\circ$ tiles are taken from the ETOPO-5 data set of the *National Geophysical Data Center* [1988]. Average values of density, V_p , and V_s for the water layer are chosen to be 1.02 g/cm^3 , 1.50 km/s , and 0 km/s , respectively, while the values for the ice layer are 0.92 g/cm^3 , 3.81 km/s , and 1.94 km/s , respectively [Bass, 1995]. The thickness of pack ice in the Arctic and Antarctic oceans can vary greatly (due to both seasonal and local changes). Comprehensive surveys of ice thickness have not been carried out, but the regional thickness probably does not exceed 10 m [e.g., Kovacs *et al.*, 1995]. Therefore pack ice is ignored in our model.

4. Sedimentary Layers

An accurate description of the global distribution of sediments and the determination of their physical properties was a

major aspect of this study. This was deemed necessary in view of the low elastic velocities and densities of some sedimentary basins that result in these basins having a major effect on all geophysical measurements. This information was compiled on a $5^\circ \times 5^\circ$ grid from the published literature (Table 1). Continental sedimentary thickness was compiled using global atlases, continent-scale summaries, and individual reports. It was necessary to describe sedimentary accumulations in two layers, corresponding to “soft” and “hard” sediments. On continents, the P wave velocity is $2.0\text{--}3.0 \text{ km/s}$ in unconsolidated (soft) sediments and is $4.0\text{--}5.3 \text{ km/s}$ in the consolidated (hard) layer. The thickness of sediments on the continents varies from zero to more than 20 km; the vast platform regions are covered by 1–5 km of soft and hard sediments (Plate 1c). In many regions, metamorphosed Paleozoic sediments are included as part of the upper crystalline crust on the basis of their seismic velocity

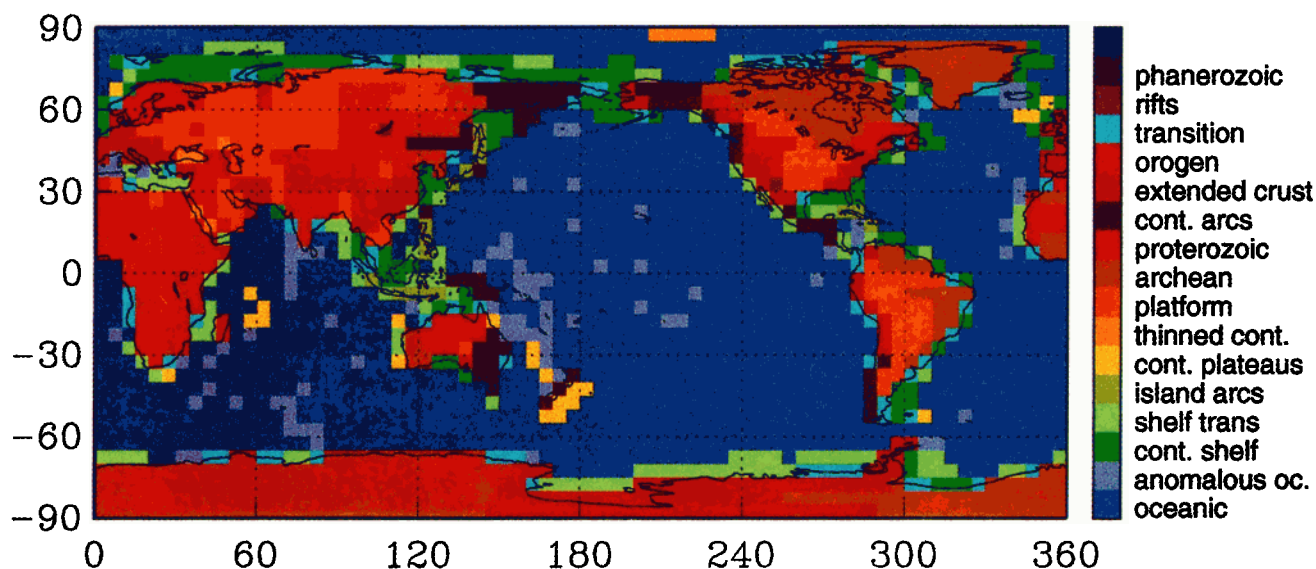


Plate 1a. Global distribution of primary crustal types used to construct the model CRUST 5.1. The crustal structure in unmeasured regions has been extrapolated using statistical averages of regions of similar tectonic setting (compare models in Figure 2).

(>5.0 km/s) and density (>2.5 g/cm³). The densities of the continental sediments were estimated using the velocity/density relationship of Ludwig *et al.* [1970].

The sedimentary layers in the oceans were compiled from digital data files, maps, and atlases (Table 1). The thickness of oceanic sediments is determined in sonobuoy experiments from acoustic two-way travel times by applying an x^2-t^2 method [Le Pichon *et al.*, 1968]. The mean velocity in a sedimentary layer is easily recovered from the sediment thickness using regression formulae such as those given by Ludwig and Houtz [1979]. Vast portions of the oceanic crust are covered with 150 m or less of soft sediments. Young oceanic crust has little or no sedimentary cover, and older crust, particularly at

low latitudes, has the greatest sedimentary thickness (500 m). Sound velocities in these mostly unconsolidated sediments vary greatly with depth and are usually low. Tucholke [1986] found sediment velocities ranging from 1.45 km/s at the surface to 3.5 km/s at a depth of 3.7 km. In general, oceanic sediments are too thin to justify a detailed description of their variations in physical properties when working on a global scale. Therefore, for sedimentary sequences less than 2 km thick we simply represent the whole sequence by one layer. In our model, ocean sediments less than 700 m thick have an average velocity of 2.0 km/s in equatorial latitudes (due to greater calcareous content) and 1.75 km/s elsewhere. This average velocity increases with thicker sedimentary cover. When oceanic sedi-

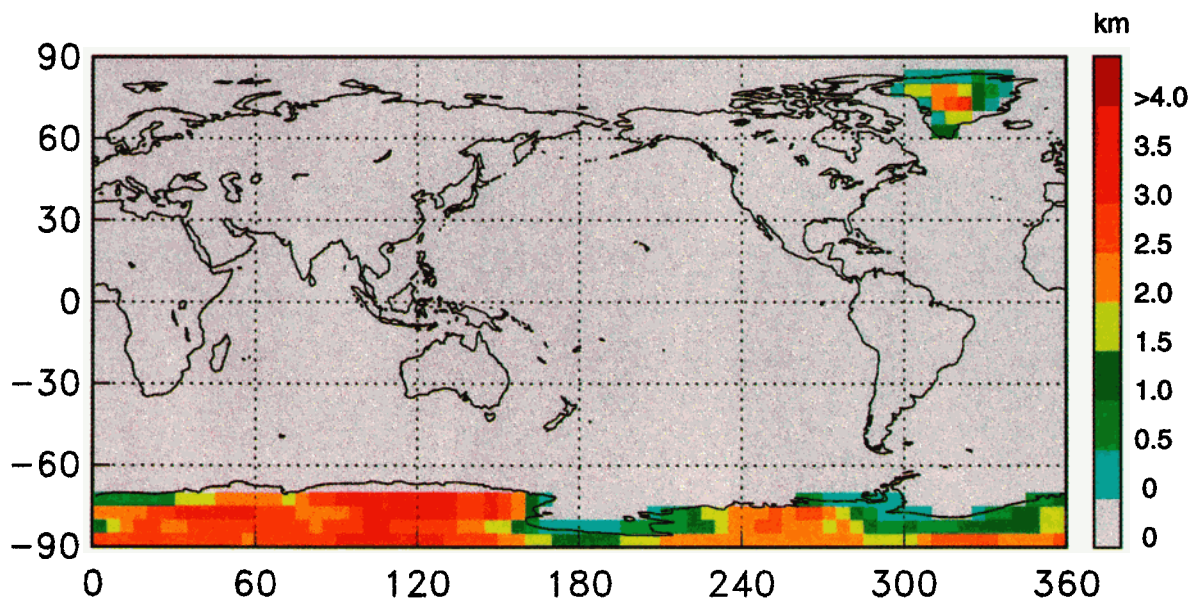


Plate 1b. Global distribution of the thickness of the ice layer (layer 1; layer 2 is bathymetry taken from the database ETOPO-5).

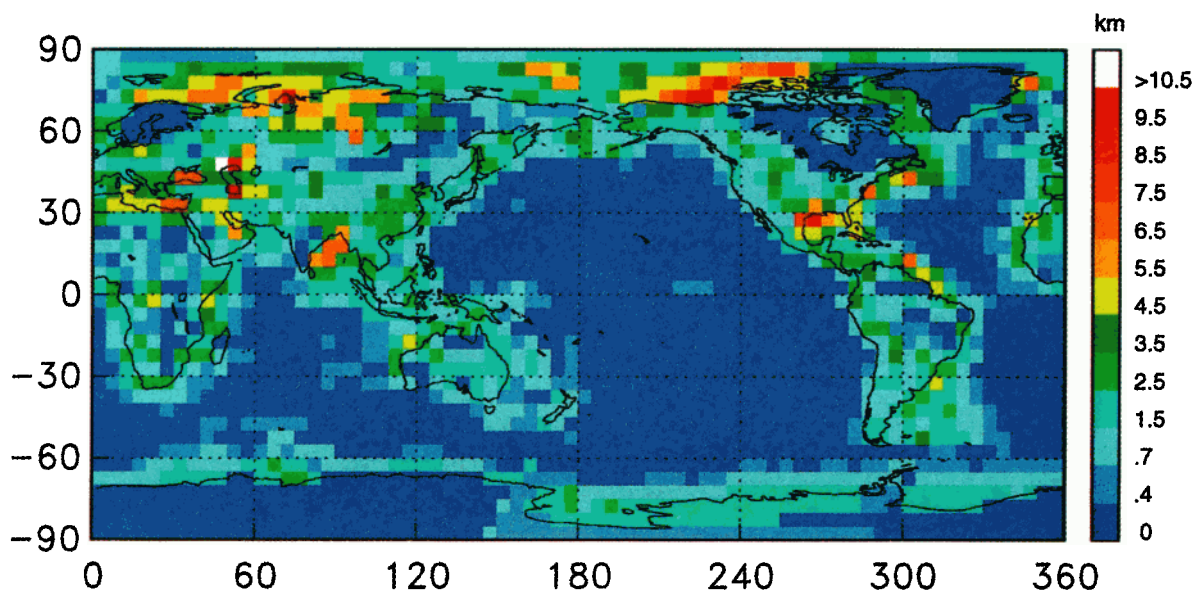


Plate 1c. Global distribution of sediment thickness (summation of layers 3 and 4, soft and hard sediments). Sediment thickness ranges from 0 m (exposed basement) to 150 m (largest ocean basins) to 12 km. The large ($5^\circ \times 5^\circ$) grid size results in significant smoothing of this parameter which can locally exceed 20 km. Large-scale regions with sedimentary accumulations in excess of 10 km are mostly found at continental margins and within intracontinental depressions, such as the Black Sea and the Caspian Depression.

ment thickness exceeds 2 km, two layers are used. The mean velocity of each layer is chosen such that the calculated two-way travel times match the measured values. Note that this division into two layers is somewhat arbitrary and does not reflect a division into unconsolidated and consolidated sediments as usually defined in the literature [e.g., *Ewing and Nafe, 1966*]. Density and shear velocities for oceanic sediments have been calculated using regression lines given by *Hamilton [1976, 1978]*. Poisson's ratio in oceanic sediments can be rather high

(up to 0.44 for the shallow, water-saturated sediments) which means that shear velocities can be very low.

Some of the thickest sedimentary accumulations occur at continental margins and inland seas. For example, sediment thickness in the Bay of Bengal and Arctic Ocean is greater than 10 km locally, and the Red Sea and Mediterranean are underlain by thick sequences of evaporites. Much of the Gulf of Mexico is also covered by thick sequences of sediments and salt deposits. Fortunately, most of these regions have been extensively

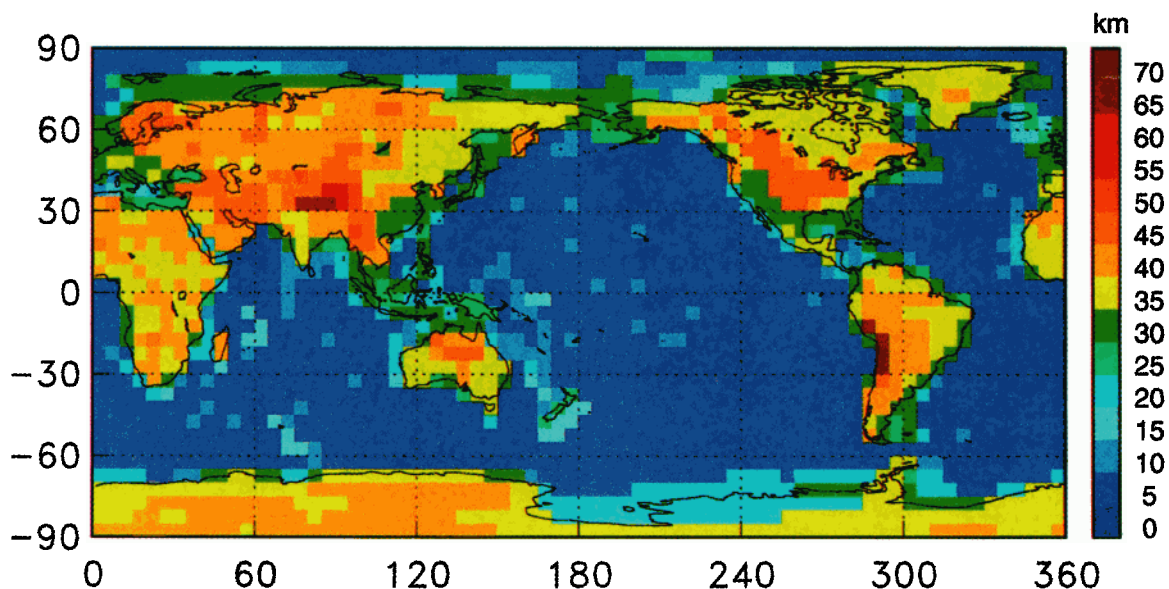


Plate 1d. Global crustal thickness, including topography above sea level but not bathymetry. The average thickness of continental crust, including shelf regions, is 38 km and varies locally from 20.5 km (extended crust) to 70 km (Tibetan Plateau).

Table 1. Sedimentary Basin Compilations and Sediment Thickness Maps

Reference	Region Covered
Heezen et al. [1977]	Indian Ocean, Red Sea
Ross [1977]	Black Sea
Ludwig and Houtz [1979]	North and South Pacific Ocean
El Shazly [1982]	Red Sea
Belousov and Pavlenkova [1984]	Eurasia
Exxon Production Research Company [1985]	global sediment map
Salvador [1986]	Gulf of Mexico
Tucholke [1986]	North Atlantic
Jackson and Oakey [1986]	Arctic Ocean
Renkin and Sclater [1988]	North Pacific Ocean
Rabinowitz et al. [1988]	Indian Ocean
Belousov et al. [1988]	Eurasia
Tucholke and Uchupi [1989a]	North Atlantic
Tucholke and Uchupi [1989b]	Mid-Atlantic
Divins and Rabinowitz [1989]	South Atlantic
Hayes [1991]	Antarctica, Southern Oceans
Norris [1993]	Hudson Bay

studied in the course of hydrocarbon exploration, and much information is available regarding the seismic structure of the sedimentary basins at continental margins [e.g., Brocher, 1995].

5. Crystalline Crust of the Continents and Their Margins

The crystalline continental crust has been parameterized in terms of three layers, in agreement with recent summaries of continental crustal structure [Meissner, 1986; Mooney and Braile, 1989; Mooney, 1989; Holbrook et al., 1992; Christensen and Mooney, 1995; Pavlenkova, 1996]. The upper crust is defined as the portion of the crust with a P wave velocity of 5.7–6.3 km/s, and the middle and lower crusts are defined as the portions of the crust with P wave velocities of 6.4–6.7 km/s and 6.8–7.4 km/s, respectively. The distribution of continental seismic refraction profiles compiled for this study is shown in Figure 1. Every effort has been made to include all reliable seismic refraction measurements. These data were compiled from the published literature and from a limited number of unpublished reports. The published literature appeared in 1948–1995 [Christensen and Mooney, 1995] and includes journal articles, monographs, and special publications such as meeting proceedings, governmental open file reports, and annual reports of research institutions. Unpublished literature primarily consists of high-quality technical reports of recent field measurements that have been issued prior to journal publication. We have not included estimates of crustal thickness from seismic reflection profiles or techniques using broadband seismic data (e.g., receiver functions) since these do not provide determinations of the P wave velocity-depth structure.

The deep structure of continental margins has been well determined using multichannel seismic reflection and refraction profiles. The results of these investigations appear in a wide range of reports, maps, and national atlases [e.g., Pakiser and Mooney, 1989; Holbrook et al., 1994; Brocher, 1995]. These regions show strong lateral variations in crustal structure; consequently, the seismic velocity structure within the $5^\circ \times 5^\circ$ tiles can only be a rough approximation to the structure at any given point.

The shear wave velocity within the crust has been determined from (1) seismic refraction measurements, where available, and (2) by converting the compressional wave model into

a shear wave model using estimated V_p/V_s ratios for each crustal layer determined from field and laboratory measurements [Christensen, 1996]. The estimation of crustal density from compressional wave velocity is nonunique, as attested to by the numerous studies that have attempted to estimate crustal density from combined modeling of seismic and gravity data. However, since we are describing $5^\circ \times 5^\circ$ cells, small-scale density inhomogeneities are less important. For the estimation of density at depth we use the linear regression lines of Christensen and Mooney [1995].

6. Crystalline Oceanic Crust

Seismic refraction studies show that the oceanic crust is 6–7 km thick. The crystalline portion of our average oceanic model is a simple three-layer approximation of previously published standard models [Spudich and Orcutt [1980], Orcutt [1987], White et al. [1992], Christensen and Salisbury [1975], and data distribution in Figure 1). The first layer of the three-layer crystalline crust (oceanic layer 2 [Raitt, 1966]) includes pillow basalts and sheeted dikes. This layer has an average V_p velocity of 5.0 km/s. The lower two layers represent the gabbroic layer with a slightly positive velocity gradient (known as oceanic layer 3). Oceanic layer 3 was subdivided into two layers to conform to the three-layer description of the continental crystalline crust. The P wave velocities of these layers are 6.6 and 7.1 km/s. The thickness of the oceanic igneous crust is reported to be fairly uniform. In our model it is chosen to be 6.5 km, although recently, White et al. [1992] suggested a slightly larger value (7.2 km). Crustal thickness is significantly less along fractures zones [Orcutt, 1987; White et al., 1992], and crustal velocities are lower as well; upper mantle seismic velocities are often found at depths of 2–3 km, where oceanic layer 3 appears to be missing. Fracture zones are 40–80 km apart in the Atlantic Ocean, which causes significant small-scale lateral heterogeneity. These fracture zones also produce a strong positive anomaly in the gravity signal, in contrast to those in the Pacific Ocean. The total width of these fracture zones are 10 to 30 km (D. K. Blackman, personal communication, 1996) so that, in some areas, the weighted average crustal thickness might be decreased by several hundred meters, even on a scale of $5^\circ \times 5^\circ$. Since global variations in the thickness of oceanic crust are not known with sufficient detail at present, we have chosen to neglect this effect in this edition of the crustal model. Anomalous thin crust can also be found near very slow spreading ridges and in regions adjacent to some continental margins. These anomalies are significant in a high-resolution global model but tend to be averaged out in a model on a $5^\circ \times 5^\circ$ scale. There is no evidence that crustal thickness varies greatly with spreading rate [Chen, 1992] except at slow spreading ridges [White et al., 1992]. Crustal thickness also does not appear to change significantly with lithospheric age [see Tani-moto, 1995, Table 3] although the crust might be thinner within a few kilometers of the mid-ocean ridges. Grevenmeyer and Weigel [1996] have also found age-dependent seismic velocities for crust younger than about 5 Ma, but these effects are too small-scale to be included in the present model.

7. Anomalous Crust: Oceanic Plateaus, Hotspots, and Rifts

The thickness of the igneous section of oceanic crust can increase to 10 km or more in the vicinity of mantle plumes

(e.g., Iceland, Hawaii, Cape Verdes, Kerguelen) or plateaus. Many of these locations have islands and can be associated with hotspots [Phipps Morgan *et al.*, 1995]. Some of these areas are large enough to dominate the structure of at least one $5^\circ \times 5^\circ$ cell in a global map. White *et al.* [1992] derive crustal thickness by estimating melt volumes within such regions. They find that the largest melt volumes occur on aseismic ridges directly above the central rising core of mantle plumes. Crustal thickness is estimated to be about 20 km at these locations. This is also observed by Detrick and Watts [1979], who find that the thickness of some aseismic ridges such as the Walvis and the Ninety-East Ridge varies from 15 to 25 km. Following White *et al.* [1992], we distinguish between oceanic plateaus with 10 and 20 km thick crystalline crust. Some of the largest oceanic plateaus (such as the Caribbean Plateau, Ontong Java plateau, and Mid-Pacific Mountains) are located on thermal swells where the bathymetry indicates large-scale upwelling. Schubert and Sandwell [1989] and Abbott *et al.* [1997] estimated the volume and crustal thickness from bathymetric data by assuming isostatic compensation for these plateaus. The seismic structure of many of these plateaus, however, is still unknown. The crust of the Ontong Java plateau has seismic velocities that are typical for oceanic crust [Butler, 1986]. More recent studies reveal that the crust in this area can be as thick as 35 km locally [Gladczenko *et al.*, 1996]. Dredging indicates that other plateaus are clearly of continental character (such as the Falkland Plateau, Lord Howe Rise, and parts of Kerguelen, Seychelles, and Arctic Ridges), and Precambrian granites are exposed on the Seychelles Ridge. We use results reported by Nur and Ben-Avraham [1982], Schubert and Sandwell [1989], and White *et al.* [1992] to estimate the crustal thickness of these plateaus in our model.

The interaction of mantle plumes with continental crust appears to be rather complicated, and a regular pattern of crustal thickening or thinning is not observed. Plume interaction with continental crust is probably most profound in the Afar Triangle, Red Sea, and East African Rift system where substantial crustal thinning is observed [Voggenreiter *et al.*, 1988; Mechie *et al.*, 1994]. The thin crust of the Afar Triangle is most probably due to extension associated with the rifting process in the Red Sea rather than solely due to plume interaction. Anomalously thin crust has also been found in other rift systems such as the East African Rift, Baikal Rift, Rhine Graben, and Rio Grande Rift, but many of these anomalies are too local to be significant on a $5^\circ \times 5^\circ$ scale.

8. Global Crustal Thickness

The crustal thickness of our model is shown in Plate 1d, where the bathymetry (i.e., water layer) is excluded. In areas with good data coverage, crustal thickness is very similar to existing continental-scale models (e.g., compare Eurasia with the model of Meissner [1986] and North America with the model of Mooney and Braile [1989]). In the oceans, tiles with unusually thick crust correspond to the locations of the largest plateaus. Most of these areas have not been accounted for in previous models. There is also generally good agreement with the crustal thickness of model 3SMAC of Nataf and Ricard [1996], who used different data sources for their compilation. The largest differences between their model and ours occur where constraints from seismic refraction data are sparse (e.g., Africa, Greenland, and Antarctica).

Figure 4 shows one-dimensional (1-D) crustal models of

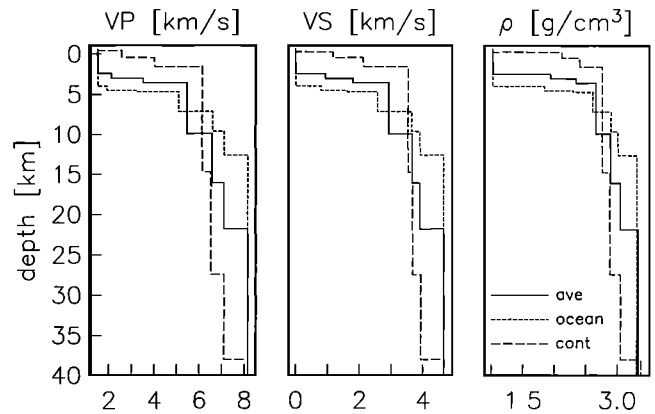


Figure 4. Depth profiles of seismic velocities and density from the model CRUST 5.1: average global crust (solid line), continental crust, including shelf regions (long dashed line), and oceanic regions (short dashed line). The negative velocity contrast between ice and underlying soft sediments is not shown. These simplified models illustrate the contrast between oceanic and continental crust that produces a strong signal in surface wave dispersion maps.

seismic velocity and density for the whole globe, for continents only (including shelf regions), and for oceans only. The mean Moho depths (with respect to sea level) are 21.8 km (global), 38.0 km (continents), and 12.6 km (oceans, including the water layer of 4.0 km average thickness). As can be seen in Figure 5a and 5b, the total crustal thickness is clearly bimodal, and in comparison to the crustal thickness model of Soller *et al.* [1982] our model has substantially higher values for continental regions. The Moho in our model is located at greater depth in some areas, especially those with poor data coverage such as Africa and South America (Figure 6). Our crustal thickness (40 km) for the vast shield areas of Africa and South America is in excellent agreement with the global average for shield areas (Figure 3a), whereas the thin (30 km) crust in the model of Soller *et al.* [1982] is clearly inconsistent with these statistics. The data coverage in Australia has increased tremendously since the publication of Soller *et al.* [1982], and our model displays a slightly deeper (by ~ 5 km) Moho. In northeastern Eurasia the Moho lies substantially deeper in CRUST 5.1 (as it does in model 3SMAC of Nataf and Ricard [1996]) than in the model of Soller *et al.* [1982]. In this part of the continent the Moho depth is constrained quite well by recently released data so that, again, we have more confidence in our model. On the other hand, based on much new data, the Moho in all of southern Eurasia is shallower in our model than in that of Soller *et al.*, sometimes by over 10 km. Again, our model agrees quite well with 3SMAC, especially in Southeast Asia. The crust in our model is also slightly thinner in North America, where our map is in close agreement with that of Mooney and Braile [1989].

Large local differences in the oceans are found in the Coral Sea (northeast of Australia) and along the Tonga-Kermadec trench. For the Coral Sea, Soller *et al.* [1982] refer to results reported by Shor [1967] and Ewing *et al.* [1970]. Shor [1967] reports the Moho at 19 km depth along a profile lying immediately south of the Coral Sea Basin, which has normal oceanic crust [Ewing *et al.*, 1970]. North of the Queensland plateau, Shor [1967] also reports a significantly thicker crust. However, the contour lines in this area are rather uncertain and are

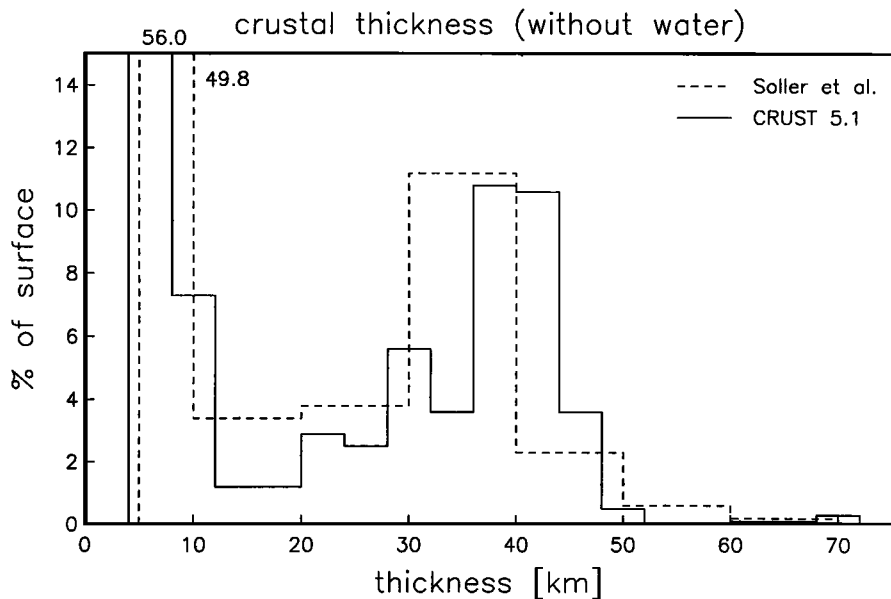


Figure 5a. Histograms of percent surface area versus crustal thickness for the model CRUST 5.1 (Plate 1d) and the model of *Soller et al.* [1982]. The counts were performed with an equal-area grid parameterization, and the numbers are given as a fraction of the global surface area in percent. Also shown is the histogram for the crustal thickness model of *Soller et al.* [1982]. While the thickness of most of the continental crust is in the 36–44 km range in CRUST 5.1, the thickness is clearly less (30–40 km) in the model of *Soller et al.* [1982]. The average Moho depth (with respect to sea level) beneath continents is 38 km in CRUST 5.1, while it is 35 km in the model of *Soller et al.* [1982].

probably overestimated by *Soller et al.* [1982], who specified 25 km as the crustal thickness. *Shor et al.* [1971] report crustal thicknesses between 11 and 15 km along portions of the Tonga-Kermadec trench, which may indicate a significant crustal thickening on a $5^\circ \times 5^\circ$ scale. The regional extent of this area of thicker oceanic crust is unknown and thus has not been included in our model.

9. Uppermost Mantle

The P wave velocity of the uppermost mantle (P_n) has been well determined beneath the continents and oceans from seis-

mic refraction measurements. For the uppermost mantle we assign a mean seismic velocity to each tile. The average P_n velocity beneath continent is 8.09 ± 0.20 km/s [*Christensen and Mooney, 1995*], and the average oceanic P_n velocity is 8.15 ± 0.31 km/s [*Christensen and Salisbury, 1975*]. In our model the P_n velocity ranges from 7.8 km/s for regions of high heat flow up to 8.2 km/s under shields and platforms. This variation (7.8–8.2 km/s) represents less than half the range in seismic velocity reported for individual seismic refraction profiles (7.6–8.6 km/s). Reliable S wave velocity determinations for the uppermost mantle (S_n) are less common but are generally

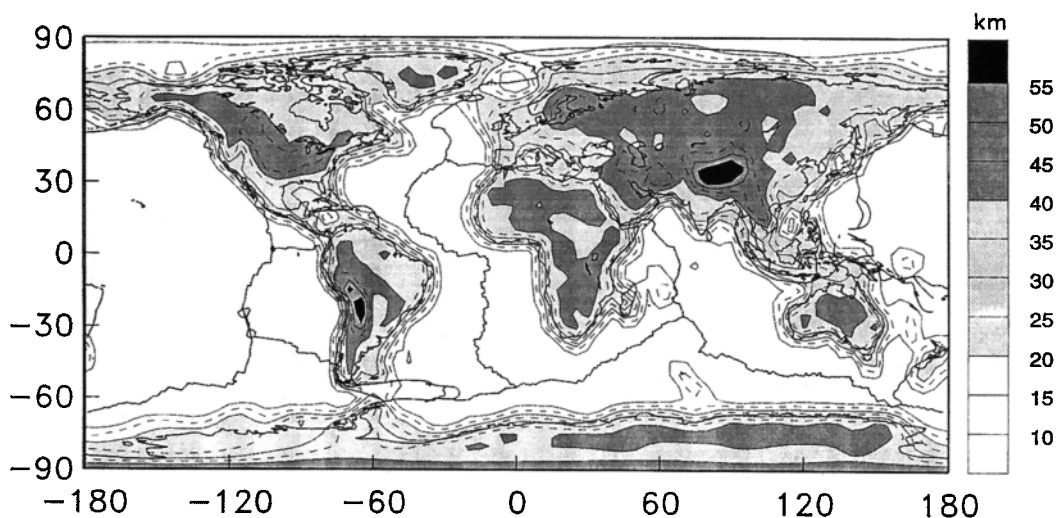


Figure 5b. Spherical harmonic expansion of the crustal thickness of CRUST 5.1 (Plate 1d). The expansion was truncated at harmonic degree 50. The solid contour lines indicate 10 km steps, while the dashed lines indicate 5 km steps.

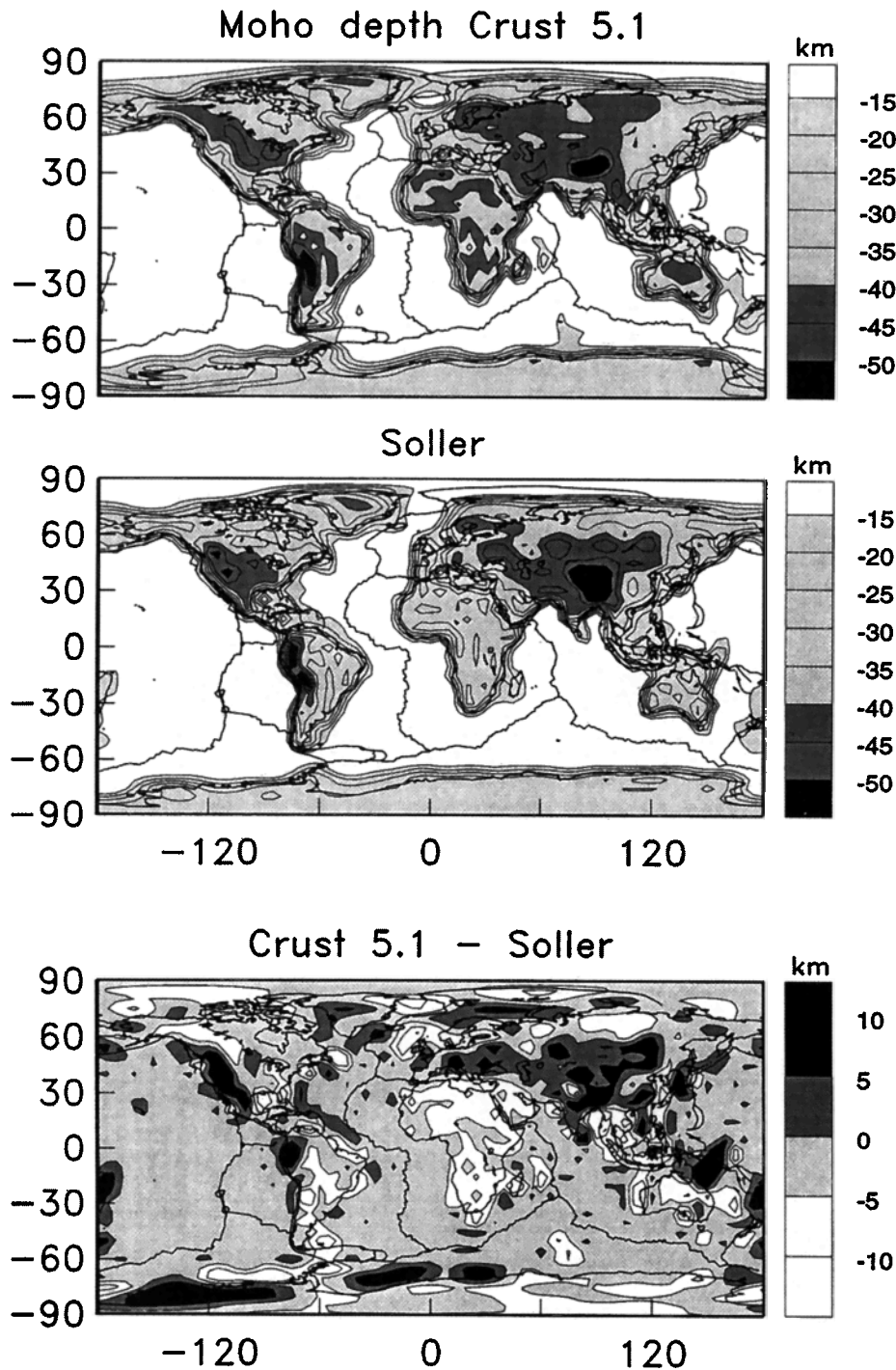


Figure 6. Spherical harmonic expansions of (top) the Moho depth (in kilometers with respect to sea level) of CRUST 5.1 and (middle) that of *Soller et al.* [1982]. The expansions were truncated at harmonic degree 36. (bottom) Large-scale differences of several kilometers in Africa and Antarctica and small-scale differences of over 10 km in southeastern Eurasia, the North American west coast, the Coral Sea, and along the Tonga-Kermadec trench.

consistent with a Poisson's ratio of ~ 0.26 . This value, which we have adopted, agrees with that derived from the assumed upper mantle composition of olivine and pyroxene [Christensen, 1996].

10. Crustal Model and Mantle Tomography

Seismic tomography has been extensively used in various forms to determine the deviations from a purely radial depen-

dence of seismic velocities within the Earth's mantle. Surface wave and free oscillation data have been used to determine the upper mantle shear wave velocity structure [e.g., Masters et al., 1982; Woodhouse and Dziewonski, 1984; Montagner and Tanimoto, 1991; Trampert and Woodhouse, 1995]. Body wave arrivals reported to the International Seismological Centre (ISC), or specially picked from seismic records, have been used to determine the *P* wave and *S* wave structure both on global and

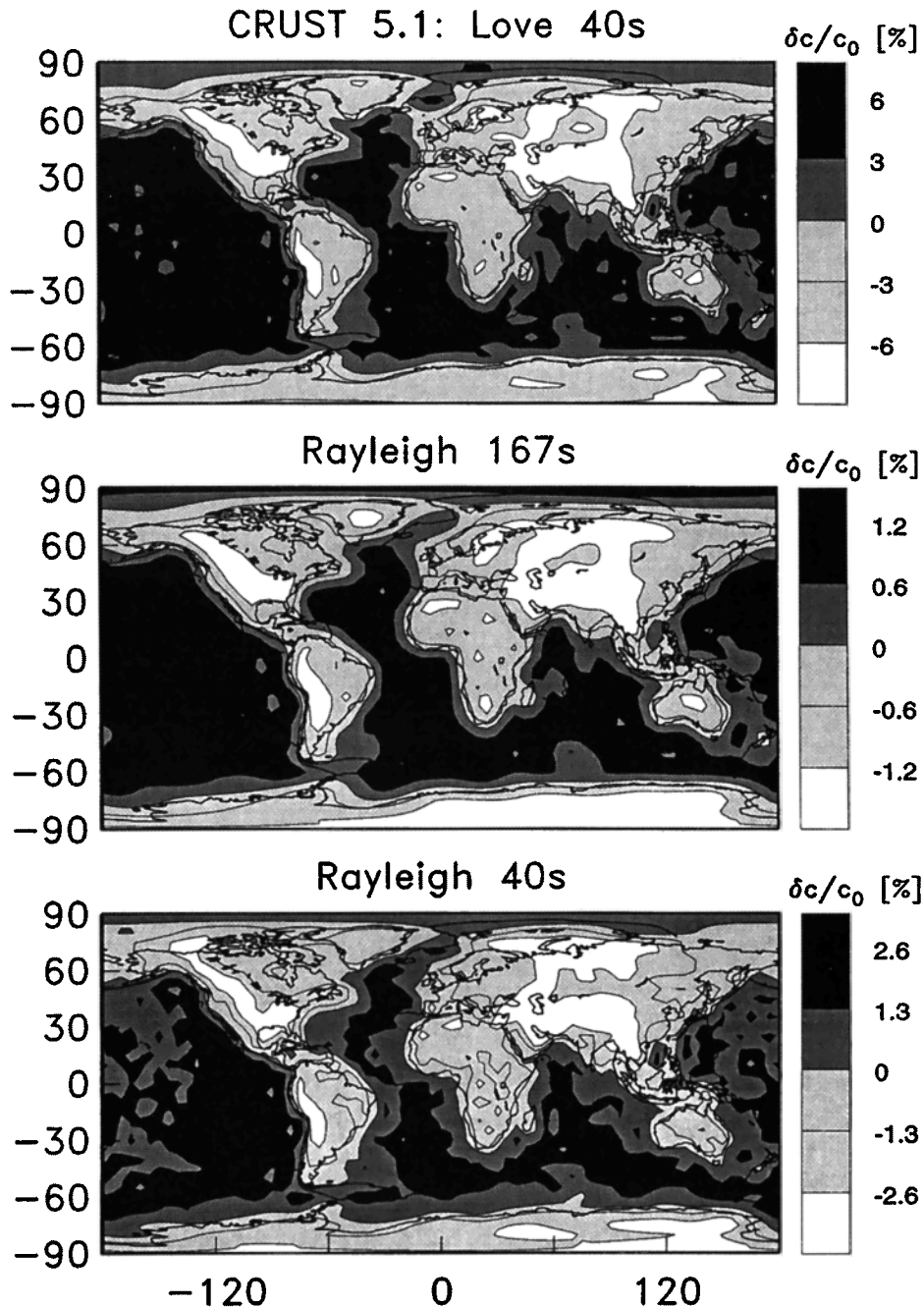


Figure 7. Spherical harmonic expansion of the crustal correction for global surface wave phase velocity maps, calculated for CRUST 5.1. The maps are truncated at the same harmonic degree (l) as the observed maps shown in the next figures. The truncation levels are $l = 24$ at 167 s and $l = 36$ at 40 s. The maps show phase velocity perturbation in percent; the global average of CRUST 5.1 has been removed.

regional scales [e.g., *Dziewonski, 1984; Inoue et al., 1990; Woodward and Masters, 1991; Pulliam et al., 1993; Zielhuis and Nolet, 1994; Grand, 1994; Vasco et al., 1995; Masters et al., 1996; Alsina et al., 1996*]. For the majority of these studies the crust has a significant effect on the observed seismic data, but at the same time, it is too thin to be resolved by these studies. Most authors handle this by applying an assumed “crustal correction” to the data before inverting for mantle structure. Since the inversion techniques can erroneously map crustal structure down to great depth, the application of accurate crustal corrections to the data sets is extremely important.

In Figure 7 we show the effect of our model on global surface wave dispersion. We will concentrate on effects on phase velocity (not group velocity) in the following. Since surface waves are sensitive to V_p , V_s , and density, a model prescribing all these parameters is essential. When calculating the crustal corrections for global maps of phase velocity, we ignore the lateral variations of V_p , V_s , and density as specified in layer 8 (uppermost mantle) of CRUST 5.1 so that anomalies displayed in the maps are caused only by variations within the crust itself. For the mantle we use the reference 1-D preliminary reference Earth model (PREM) [*Dziewonski and Ander-*

son, 1981]. Global surface wave phase velocity maps are commonly expanded in surface spherical harmonics. We adopt this parameterization and truncate the harmonic expansions as specified in the individual figure captions. For plotting purposes, the spherical averages of the maps have been removed. Crustal structure has the greatest effect on short-period surface waves. This can be seen in Figure 7 where the peak-to-peak amplitude in phase velocity anomaly for Rayleigh waves at 40 s is about twice as large as that at 167 s. For Love waves the crustal effect is more than twice that of Rayleigh waves at the same period. Love waves at 40 s are most sensitive to the S wave velocity structure in the uppermost 60 km (Figure 8) (they are also sensitive to density in the same depth range, although to a much lesser extent). Rayleigh waves at these periods are primarily sensitive to uppermost mantle structure. The sensitivity kernel for S wave velocity peaks at about 60 km and has a minimum at 20 km depth. However, Rayleigh waves at 40 s are also quite sensitive to variations of P wave velocity within the shallowmost layers of the crust. Hence the large thick sedimentary basins (e.g., in the Arctic ocean or the Gulf of Mexico) cause significant phase velocity anomalies which are not seen in the maps for Love waves at the same period.

When expanded in surface spherical harmonics, continent-ocean-type functions (such as our crustal model) are dominated by harmonic degrees $l = 1$ through 5, but the amplitude is greatest at the first harmonic degree. Surface wave phase velocity maps that have had the crustal signal removed are dominated by contributions from the first harmonic degree in a wide range of periods. Hence it is very important to obtain an accurate estimate of the structural contrast between continental and oceanic crust in order to ultimately avoid erroneous

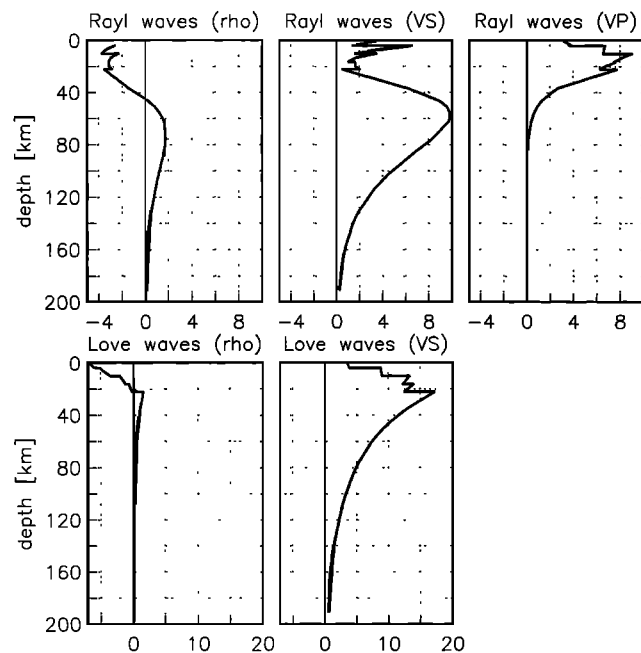


Figure 8. Sensitivity kernels for Rayleigh and Love waves at a period of 40 s. Kernels are shown for density (ρ) and S wave and P wave velocities. Love waves are insensitive to variations in V_p and are primarily sensitive to S wave structure in the upper 60 km. Sensitivity is greatest above 40 km; hence 40 s Love waves mainly sample the crust. Note, however, that the sensitivity to upper mantle structure below 60 km is still significant.

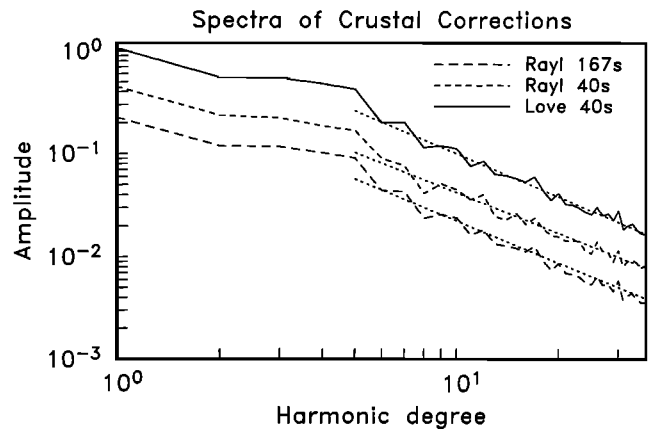


Figure 9. Amplitude spectra of the three maps shown in Figure 7. The amplitude spectra are normalized so that the spectrum of a spike function would be flat. With this normalization, the roll-off of the spectra is roughly proportional to l^a . The parameter a is determined by fitting straight lines to the spectra at harmonic degrees above $l = 5$ and is -1.19 for 40 s Rayleigh waves and -1.34 for 167 s Rayleigh and 40 s Love waves.

mapping of the continent-ocean function into greater depth in the upper mantle. At higher harmonic degrees the spectra of the crustal corrections roll off roughly as l^a , where a is a negative number between -1 and -2 . To illustrate this behavior, we plot the amplitude spectra of the crustal corrections of Figure 7 on a double-logarithmic scale (Figure 9). The roll-off can then be fit by straight lines where the slope of the lines is a . We find that this parameter is fairly uniform ($a = -1.35$) for both Love and Rayleigh in the period range between 167 s and 40 s. For Rayleigh waves at 40 s, the roll-off is slightly less ($a = -1.19$), probably due to the increased sensitivity to the small-scale variations of the P wave velocity in the thick sedimentary basins.

Figures 10 and 11 show examples of the global phase velocity maps of *Laske and Masters [1996]* and *Ekström et al. [1997]* before and after removal of the perturbations due to the crust. For long-period surface waves, lateral phase velocity variations caused by crustal heterogeneities are relatively small. Nevertheless, the crustal correction actually increases the variance of the observed phase velocity. The peak-to-peak amplitude for Rayleigh waves at 167 s is larger after the correction by a factor of roughly 1.3 (Figures 10a and 10b). The increase in variance is caused by the fact that the signal from the crust and the uppermost mantle are often anticorrelated; for example, shields have large crustal thickness and low crustal velocities (as compared to the oceans at the same depth) but high velocities in the upper mantle. Obviously, the application of a crustal correction is important for interpreting these long-period surface wave data. However, the fine details of the crustal model used do not appear to be crucial.

The situation is quite different for short-period surface waves. In this case, for continental paths, Love waves with a period of 40 s are dominantly sensitive to crustal structure. In fact, Love wave phase velocities at shorter periods [e.g., *Ekström et al., 1997*] could be used in the future to further refine crustal models where no refraction seismic data are available. The signal in the map (Figure 11a) is greatly decreased (by a factor of 1.7) by the crustal correction (Figure 11c). The re-

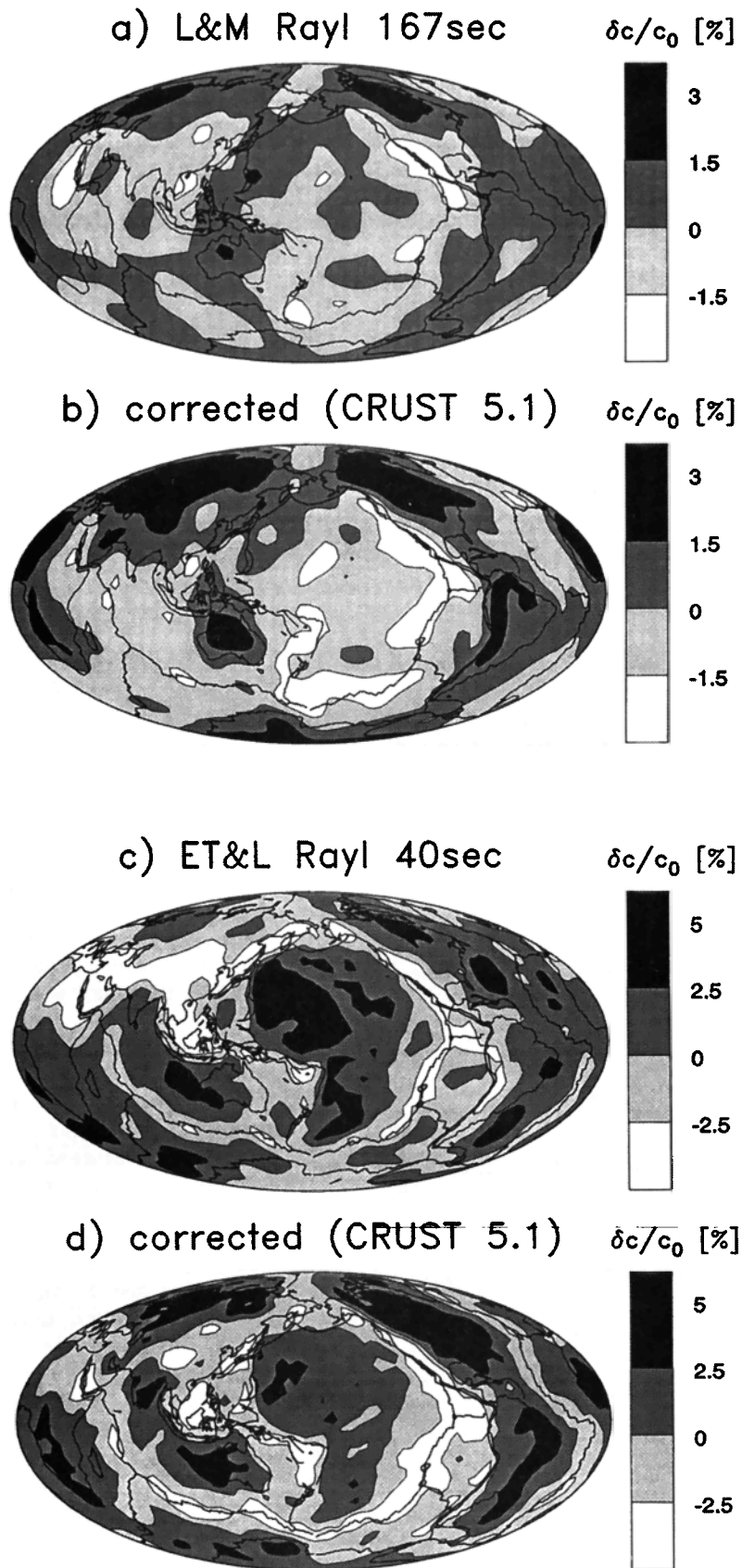


Figure 10. (a) Observed phase velocity map for Rayleigh waves at 167 s (“L&M” [Laske and Masters, 1996]). The phase velocity perturbation typically varies between -1.5% and 1.5% . (b) After the correction for crustal signal, these variations are substantially larger. (c) Observed phase velocity map for Rayleigh waves at 40 s (“ET&L”) [Ekström et al., 1997]. (d) Map corrected for crustal signal. The crust correction at this period does not increase the variance but redistributes the anomalies.

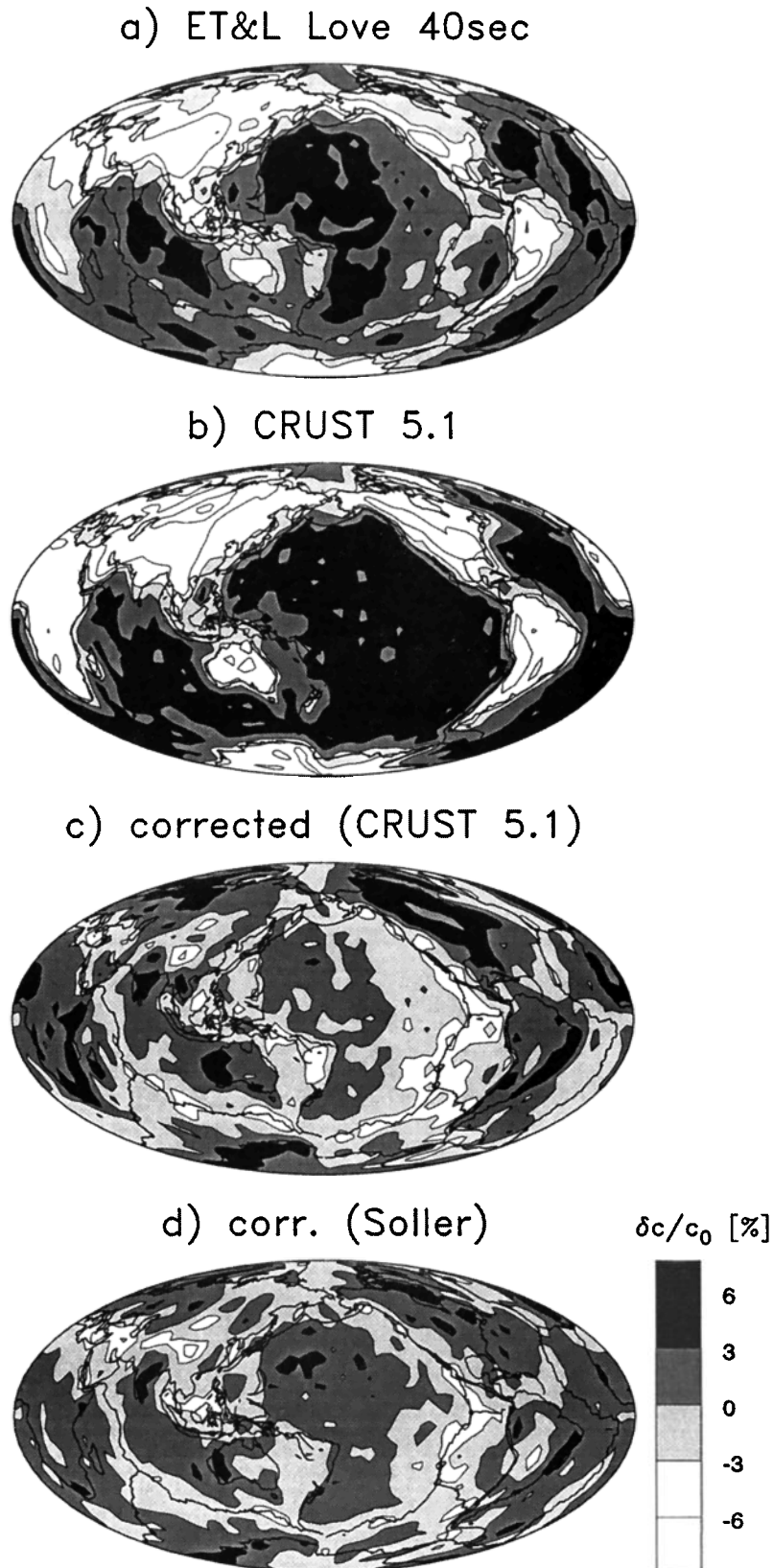


Figure 11. (a) Observed phase velocity map for Love waves at 40 s [Ekström *et al.*, 1997]. (b) Calculated crustal signal in the phase velocity map as predicted by our crustal model CRUST 5.1. (c) Observed phase velocity map (Figure 11a) corrected for crustal signal for the model CRUST 5.1 (Figure 11b). (d) Observed phase velocity map (Figure 11a) corrected for the crustal signal using crustal thicknesses from Soller *et al.* [1982] (see text for details). Note that while Figure 11c displays pronounced high-velocity anomalies under shields, these anomalies are much smaller in Figure 11d.

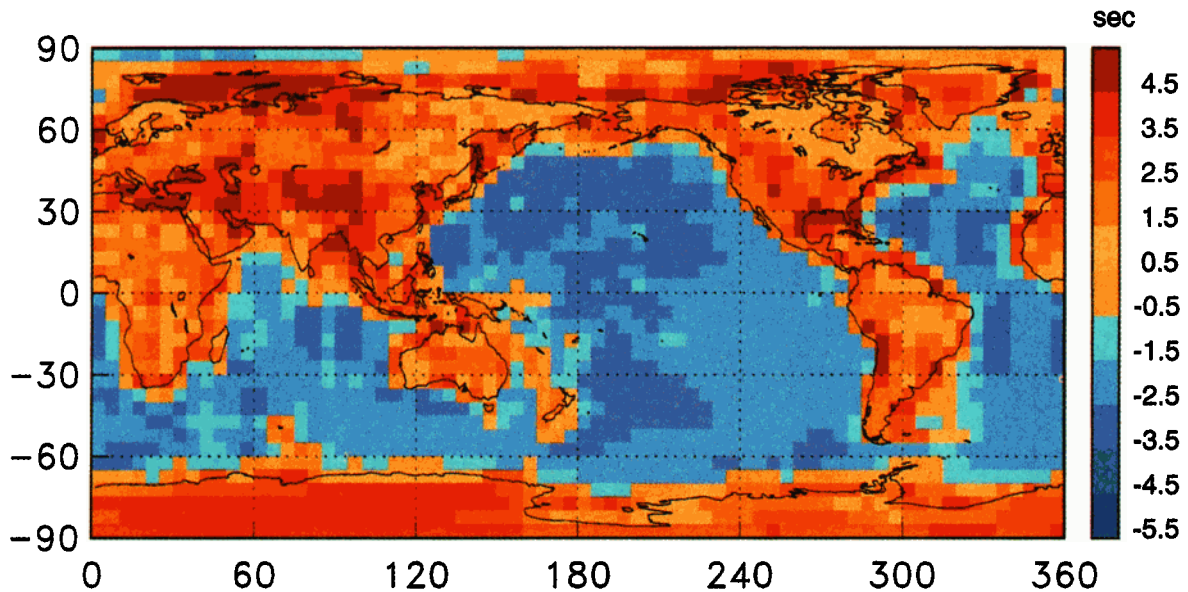


Plate 2. Two-way S wave travel time anomalies (vertical incidence assumed) as calculated with the model CRUST 5.1. The travel times are given as anomalies with respect to a global “average crust” of 21 km thickness and average shear wave velocity of 3.4 km/s. The crustal correction is large, ranging from +4.5 s to -5.5 s.

maining signal is primarily produced by an age-dependent cooling of the oceanic lithosphere, which is not included in the crustal model. For comparison, we also show the crustal correction for a model [Smith, 1989] used in earlier studies (Figure 11d). This model includes the Moho variation of Soller *et al.* [1982] and estimated average seismic velocities and densities for continents and oceans [Smith, 1989] (referred to as the “Soller model” hereafter). It is interesting to note that the resulting map (Figure 11d) does not display the pronounced high-velocity regions beneath the shields that CRUST 5.1 pro-

duces, and there are many other regional differences. Since 40 s Love waves are sensitive to upper mantle structure below 60 km, it is to be expected that the high-velocity mantle beneath shields will be clearly evident in the corrected maps. Based on this comparison, we are confident that the crustal corrections from CRUST 5.1 are more accurate than the corrections derived from the Soller model. It is also worth noting that the spectra of the crustal corrections of CRUST 5.1 and the Soller model are similar in shape but that the corrections of CRUST 5.1 have significantly larger amplitudes at harmonic

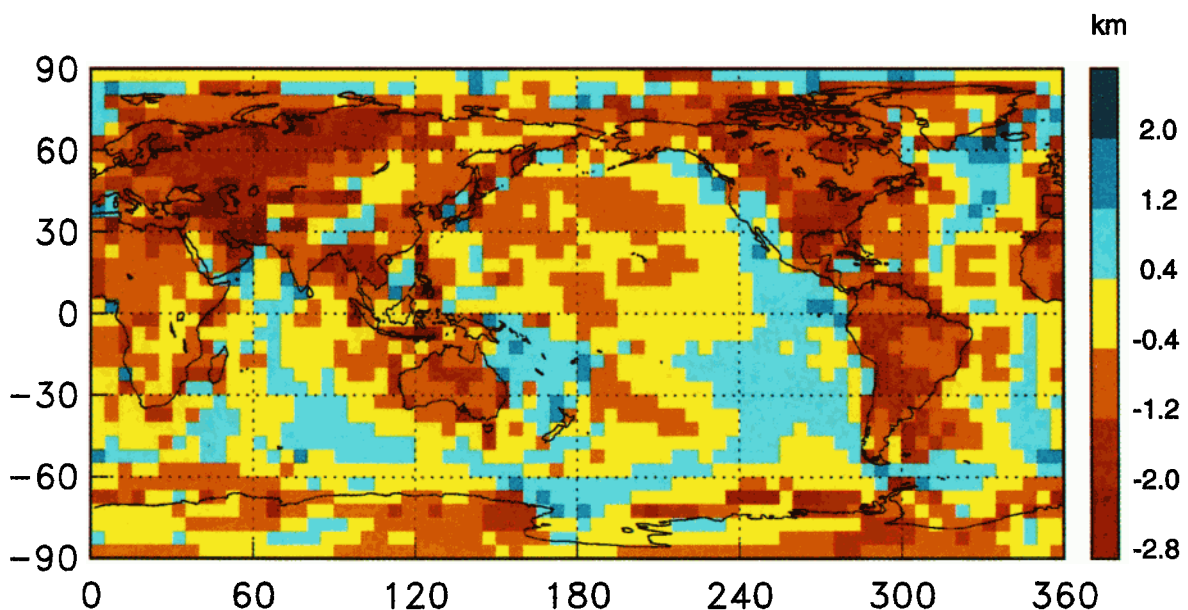


Plate 3. Residual isostatic topography (in kilometers) calculated from observed topography (ETOPO-5) minus the topography predicted from an “isostatically balanced crust” (see text) of CRUST 5.1. The residual topography in the oceans can be explained by isostatic compensation by a cooling lithosphere. Anomalies on continents are probably caused by dense continental roots beneath the shields.

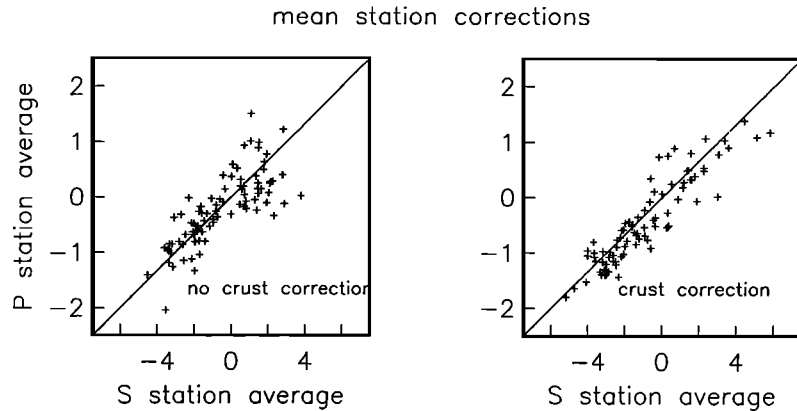


Figure 12. (left) Station means for 85 global seismic broadband stations for which we have at least 100 measurements for both S and P arrival times. (right) Crust corrections have been applied to the individual measurements before calculation of the means, and the 3:1 $S:P$ ratio characteristic of the upper mantle is more clearly shown (the crustal signal alone gives a $\sqrt{3}:1$ $S:P$ ratio).

degrees less than $l = 5$ (not shown here). The largest discrepancy is at $l = 1$ where the amplitude of CRUST 5.1 is roughly 1.5 times that of the Soller model. This discrepancy is due to the difference between the average parameters for continents and oceans in the two models. This comparison further stresses the need for accurately estimating seismic velocities and densities at even the longest-wavelength scale (i.e., the contrast in physical properties between continents and oceans).

Rayleigh waves at 40 s sample the Earth quite differently than Love waves at 40 s. As mentioned above, these waves primarily sample the S wave velocity in the upper mantle, but they are also sensitive to the shallow P wave velocity and density structure. The overall effect is that crustal corrections for 40 s Rayleigh waves (Figure 10c) do not change the variance of the anomalies in the maps but redistribute the phase velocity anomalies significantly. High velocities in the mantle beneath shields are much more pronounced after the correction, while the low-velocity anomaly extending from the Afar Triangle through China is decreased significantly (Figure 10d). After crustal correction, the previously large low-velocity anomaly around the Afar Triangle/Red Sea area is much smaller and concentrates along the Red Sea. This same behavior occurs for both Love and Rayleigh wave phase velocity maps in a large range of frequencies (down to 167 s) and indicates that the Afar Triangle/Red Sea low-velocity anomaly is mostly produced by shallow structure.

Other data sets used in global tomography are also profoundly affected by the crustal correction. In general, the gross features of these data sets (e.g., $SS-S$ differential travel times) are changed by applying a crustal correction, but most current crustal models (i.e., Soller model [Smith, 1989], 3SMAC [Nataf and Ricard, 1996], CRUST 5.1) give similar effects. As we progress to regional scales, different crustal models give quite different answers, and the accuracy of the crustal model becomes crucial. The crustal signal for two-way S wave travel times is given in Plate 2. The travel times are with respect to a global average crustal thickness of 21 km. The travel time anomalies range from over +5 s in areas of large crustal thickness and shelves with thick sedimentary accumulations to less than -4 s in the old oceans. A similar picture is obtained for P waves where the anomalies range from +2.5 s to -2.5 s. There is a strong correlation between S wave and P wave travel

time anomalies, and the scaling between S wave and P wave velocity anomalies in CRUST 5.1 is roughly $\sqrt{3}$. It is interesting to note that if we remove the crustal contribution to S and P station corrections, we find that they become much better correlated. After the removal of crustal contributions, the ratio between them is a factor of 3 (Figure 12) rather than $\sqrt{3}$. This result implies that the crust can significantly obscure the time relationship between P and S travel times in the mantle. The ratio of 3 is also observed in travel time residuals of seismic phases which sample the upper mantle [e.g., Woodward and Masters, 1991].

11. Crustal Model and Isostasy

A useful check of our model is a consideration of crustal isostasy which is sensitive to the product of crustal thickness and average crustal density. (Here we use the term “crustal isostasy” to refer to the crustal portion of lithospheric buoyancy, as evidenced by comparing observed and predicted topography. We do not calculate true isostatic equilibrium, which would require a density model for the uppermost mantle.) This comparison with crustal isostasy is particularly valuable because crustal density cannot be directly determined from seismic refraction field measurements; therefore we have relied on published empirical relationships between P wave velocity and density. We do not expect that crustal isostasy alone will closely predict the actual topography because of lateral variations in the density of the subcrustal lithosphere. Nevertheless, this comparison is very useful for identifying broad trends and cells that are clearly anomalous in either thickness or average crustal density (or both).

We have calculated the predicted topography of the Earth using our crustal model and the assumption that the crustal column alone is in isostatic equilibrium. Plate 3 shows that there is good general agreement between actual and predicted topography, with the differences generally being less than 400 m in the oceans and 1.2 km or less on continents. An earlier iteration of this calculation revealed local discrepancies of over 3 km, and an examination of these cells revealed errors in sediment velocities (and hence density) for very thick sediment accumulations. Also, it appeared that some cells with strong lateral variations in crustal structure, especially along

continental margins, had a crustal thickness that was overestimated (or density underestimated), which created errors in these cells. These discrepancies have been corrected.

The remaining residual topography in the oceans is mainly due to lateral variations in mantle structure due to the cooling of the oceanic lithosphere with age, a process that does not introduce changes in crustal thickness. Hence our crustal model does not predict the observed deepening of ocean basins with age.

The discrepancies between observed and predicted topography on continents are also largely due to lateral variations in mantle density that are not accounted for by a consideration of crustal isostasy (J. E. Vidale and W. D. Mooney, *The Earth's topography: The influence of the crust and the upper mantle*, submitted to *Geology*, 1997). Most of the cratonic regions of North America, South America, and Eurasia lie at lower elevations than predicted by crustal isostasy. This result is unexpected, as it has previously been suggested that the subcrustal lithosphere of Precambrian cratons is cold but neutrally buoyant due to an intrinsically light composition [Jordan, 1978, 1981]. Our results indicate the existence of a cold, high-density lithospheric root beneath most Precambrian cratons. Thus, while cratonic lithosphere may have a somewhat lighter composition than noncratonic lithosphere, it appears that very low mantle temperatures have the dominant effect in determining density. The cratonic crust of Africa, Greenland, and Antarctica appears to more nearly show crustal isostasy, which suggests either that these regions are not underlain by a dense lithospheric root or that some other mechanism, such as mantle convection or chemical depletion, provides excess buoyancy (Vidale and Mooney, submitted manuscript, 1997). At least for Africa, the first suggestion seems unlikely, since seismic tomographic images do reveal a high velocity root (Figures 10 and 11). Of course, this is only true if the velocity-density scaling for the African lithosphere is the same as for other continental cratons. The crust of western North America (Mexico and United States) shows higher than predicted elevations, and the excess buoyancy is almost certainly due to a thin lithosphere, as evidenced by tomographic models and high heat flow measurements.

12. Discussion

Our goal is to develop a global model for the seismic velocities (V_p and V_s) and density structure of the crust and uppermost mantle that may be used for a wide range of geophysical investigations. We have chosen a scale of $5^\circ \times 5^\circ$ for the model because this scale provides a reasonable compromise between the desire for resolution and the geographical distribution of data. The model (CRUST 5.1) is based on more complete information than previous models. Specifically, we have included (1) the thickness and physical properties of all ice and sedimentary accumulations; (2) the physical properties of normal and anomalous oceanic crust as reported in recently published syntheses of marine seismic measurements; (3) a detailed compilation of continental seismic refraction profiles; (4) statistical estimates of the crustal structure in regions without field measurements based on the average crustal structure determined for 14 standard crustal types; and (5) reliable estimates of shear wave velocity and density based on recently published empirical V_p - V_s and V_p -density relationships.

This model is useful for a broad range of applications in crustal and mantle seismology, as well as for nonseismological investigations for which crustal density is the most relevant parameter. For example, global topography may be approxi-

mated by making the simple isostatic assumption that the crust floats in a mantle of uniform density (Plate 3). This simple assumption provides a reasonable fit to the actual topography, with discrepancies primarily being due to lateral variations in mantle density.

We have evaluated the seismological effects of this model by comparing observed short-period (40 s) Love and Rayleigh wave phase velocities with those predicted by the crustal model. Such a comparison must be approached with caution since these phase velocities are also sensitive to mantle structure. With the global surface wave data currently available, it is not possible to completely isolate the crustal signal. However, this comparison indicates that our model provides a good match to the amplitude and areal extent of phase velocity anomalies that are associated with variations in the thickness of the continental crust and large sedimentary basins. We have applied the crustal correction to observed surface wave phase velocity maps to isolate those features that are due to variations in upper mantle structure. The most obvious features in these corrected maps are the age dependence of oceanic lithosphere and enhanced high velocity anomalies under shields. We also show that an important factor in mapping these features (especially at long periods) is an accurate knowledge of the contrast between continental and oceanic crustal structure.

A contour map based on CRUST 5.1 shows the global variation of crustal thickness (Figure 13). Because of the $5^\circ \times 5^\circ$ cell size, many interesting but narrow (less than about 250 km wide) features are not evident on this map. The thickest crust (more than 50 km) is found beneath the Tibetan Plateau, the Andes of South America, and southern Finland. Continental crust (including shelf regions) typically has a crustal thickness of 30–45 km, with a global average of 38 km (compare Figure 4). Vast regions of oceanic crust have an average thickness of 6–7 km (not including the water layer). A comparison with Figure 1 indicates where crustal thickness has been measured, and where it has been estimated based on tectonic province and crustal age.

There are two primary limitations to this model. The first is the cell size ($5^\circ \times 5^\circ$), which measures 550 km by 550 km at the equator. This cell size is too coarse to permit an accurate model of many important crustal features (e.g., narrow mountain belts or rifts) other than by using a weighted average to account for lateral variations within a cell. A smaller cell size, such as $2^\circ \times 2^\circ$, would provide ~ 6 times the resolution of the present model; such a cell size may be needed for many regional studies. However, we feel that the construction and thorough evaluation of a model with a cell size of $5^\circ \times 5^\circ$ is a necessary first step to finer scale models. A second limitation is the means by which we have parameterized the model. This consisted of assigning one of 139 crustal models to each of the 2592 cells. We found that this parameterization was well suited for the crystalline crust and uppermost mantle but did not provide the desired flexibility for parameterizing the thickness and physical properties of sedimentary accumulations. An alternative approach would be to parameterize the upper layers (ice, water, and sediments) by a grid and the lower layers (crystalline crust and upper mantle) by crustal types.

As global data sets become more complete and processing techniques evolve, it will be possible to better constrain a crustal model by using observations of short period surface wave dispersion [Ekström et al., 1997]. Such observations will be particularly valuable to constrain those parts of the Earth's crust where the data coverage from seismic refraction studies is

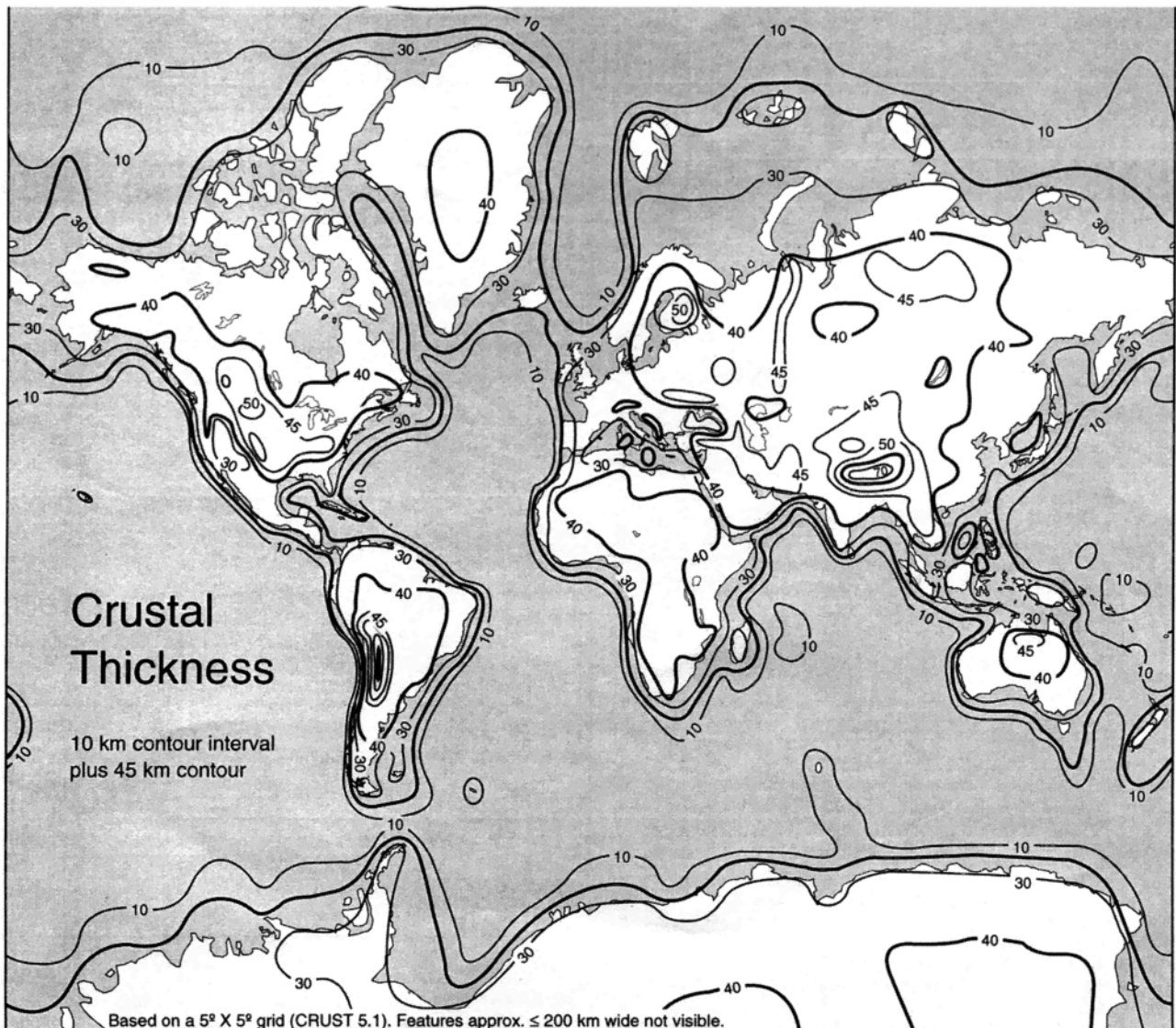


Figure 13. Mercator projection of crustal thickness from CRUST 5.1 point data (Figure 1) (85°N to 80°S latitudes). The normal ocean crust is 6–7 km thick (excluding an average water depth of 4 km). Thin crust at mid-ocean ridges and oceanic fracture zones is not visible, as these and other narrow features (such as the East African Rift) are not resolved by a map based on a 5° × 5° cell size. Stable continental regions typically have crustal thicknesses of 35–45 km, and there are few regions (at the broad scale of this map) with a crustal thickness in excess of 50 km. A comparison with Figure 1 indicates where crustal thickness has been estimated based on tectonic province and crustal age.

likely to remain poor, such as regions at high latitude. For the present, our new model, CRUST 5.1, provides the most accurate mapping of the physical properties of the crust and uppermost mantle available at a 5° × 5° scale. Further refinement will be possible as additional data become available and as additional checks are made by those who apply it to seismological and nonseismological problems. CRUST 5.1 is available from the authors at <http://quake.wr.usgs.gov/study/Crustal-Structure>, <http://mahi.ucsd.edu/Gabi>, and <ftp://carp.ucsd.edu/pub/gabi/crust>.

Acknowledgments. We would like to thank L. Gahagan and J. Sclater for providing us digital versions of the sediment thickness maps of the Pacific and South Atlantic and J.-Y. Royer for sending us

digital versions of the maps of the Indian and Southern Oceans. Many people assisted with compiling seismic refraction data: G. Chulick provided continental refraction data ("Seisprof"); M. Landes, V. O'Connor, G. Gandhok, K. Weaver, and M. Eelman assisted in the compilation of additional continental seismic refraction data; A. Egorokin, L. N. Solodilov, and N. I. Pavlenkova provided information on crustal structure from Russia; and S.-L. Li, Y.-X. Wang, and X.-C. Yuan provided information from China. We thank G. Ekström, J. Tromp, and E. Larson for making available their global surface wave dispersion maps and A. M. Dziewonski and J. R. Filson for encouragement and advice. Valuable comments on an earlier draft of this paper were provided by R. Girdler, K. Favret, K. Fuchs, G. Musacchio, R. Meissner, T. Parsons, J. Vidale, and R. L. Woodward. We also wish to thank N. I. Christensen for sending us a digital version of his CRUC tables. This research was financed by the USGS Continental Surveys Program and National Science Foundation grants EAR-94-18063 and EAR-94-05948.

References

- Abbott, D. H., R. Drury, and W. D. Mooney, Continents as lithological icebergs: The importance of buoyant lithospheric roots, *Earth Planet. Sci. Lett.*, **149**, 15–27, 1997.
- Alsina, D., R. L. Woodward, and R. K. Snieder, Shear wave velocity structure in North America from large-scale waveform inversions of surface waves, *J. Geophys. Res.*, **101**, 15,969–15,986, 1996.
- Bass, J. D., Elasticity of minerals, glasses, and melts, in *Mineral Physics and Crystallography: A Handbook of Physical Constants*, AGU Ref. Shelf, vol. 2, edited by T. J. Ahrens, pp. 45–63, AGU, Washington, D. C., 1995.
- Belousov, V. V., and N. I. Pavlenkova, The types of the Earth's crust, *J. Geodyn.*, **1**, 167–183, 1984.
- Belousov, V. V., N. Y. Kunin, V. B. Mazur, B. K. Ostistiy, and M. I. Ostrovsky, Map of the relief of the basement surface of Eurasia, scale 1:15,000,000, "Tsentrgeologia," Russ. Minist. of Geol., Moscow, 1988.
- Brocher, T. M., Deep-crustal seismology of continental margins, *U.S. Natl. Rep. Int. Union Geod. Geophys. 1991–1994*, *Rev. Geophys.*, **33**, 309–314, 1995.
- Butler, R., Regional seismic observations of the Ongtong Java Plateau and East Mariana Basin, *Mar. Geophys. Res.*, **8**, 27–38, 1986.
- Chen, Y. J., Oceanic crustal thickness versus spreading rate, *Geophys. Res. Lett.*, **19**, 753–756, 1992.
- Christensen, N. I., Seismic velocities, in *Handbook of Physical Properties of Rocks*, vol. 2, edited by R. S. Carmichael, pp. 1–228, CRC Press, Boca Raton, Fla., 1982.
- Christensen, N. I., Poisson's ratio and crustal seismology, *J. Geophys. Res.*, **101**, 3139–3156, 1996.
- Christensen, N. I., and W. D. Mooney, Seismic velocity structure and the composition of the continental crust: A global view, *J. Geophys. Res.*, **100**, 9761–9788, 1995.
- Christensen, N. I., and M. H. Salisbury, Structure and composition of the lower oceanic crust, *Rev. Geophys.*, **13**, 57–86, 1975.
- Detrick, R. S., and A. B. Watts, An analysis of isostasy in the world's oceans, 3, Aseismic ridges, *J. Geophys. Res.*, **84**, 3637–3653, 1979.
- Divins, D. L., and P. D. Rabinowitz, Thickness of sedimentary cover, Sheet 3, in *International Geology-Geophysical Atlas of the Atlantic Ocean*, edited by G. B. Udintsev, Russ. Minist. of Geol., Russ. Acad. of Sci., Moscow, 1989.
- Drewry, D. J., *Antarctica: Glaciological and Geophysical Folio*, *Polar Res. Inst., Cambridge, England*, 1983.
- Durrheim, R. J., and W. D. Mooney, Evolution of the Precambrian lithosphere: Seismological and geochemical constraints, *J. Geophys. Res.*, **99**, 15,359–15,374, 1994.
- Dziewonski, A. M., Mapping the lower mantle: Determination of lateral heterogeneity in *P* velocity up to degree and order 6, *J. Geophys. Res.*, **89**, 5929–5952, 1984.
- Dziewonski, A. M., and D. L. Anderson, Preliminary reference Earth model (PREM), *Phys. Earth Planet. Inter.*, **25**, 289–325, 1981.
- Ekström, G., J. Tromp, and E. W. F. Larson, Measurements and global models of surface wave propagation, *J. Geophys. Res.*, **102**, 8137–8157, 1997.
- El Shazly, E. M., The Red Sea region, in *The Ocean Basins and Margins*, vol. 6, *The Indian Ocean*, edited by A. E. M. Nairs and F. G. Stehli, pp. 205–252, Plenum, New York, 1982.
- Ewing, J. I., and J. E. Nafe, The unconsolidated sediments, in *The Sea*, vol. 3, *The Earth Beneath the Sea*, edited by M. N. Hill, pp. 73–84, Wiley-Interscience, New York, 1966.
- Ewing, M., L. V. Hawkins, and W. J. Ludwig, Crustal structure of the Coral Sea, *J. Geophys. Res.*, **75**, 1953–1962, 1970.
- Exxon Production Research Company, Tectonic map of the world, Am. Assoc. of Pet. Geol. Found., Tulsa, Okla., 1985.
- Gladchenko, T. P., M. F. Coffin, and O. Eldholm, Crustal structure of the Ongtong Java Plateau: Modeling of new gravity data and existing seismic data, *Eos Trans. AGU*, **77**(46), Fall Meet. Suppl., F713, 1996.
- Goodwin, A. M., *Precambrian Geology: The Dynamic Evolution of the Continental Crust*, Academic, San Diego, Calif., 1991.
- Grand, S. P., Mantle shear structure beneath the Americas and surrounding oceans, *J. Geophys. Res.*, **99**, 11,591–11,621, 1994.
- Grevemeyer, I., and W. Weigel, Seismic velocities of the uppermost igneous crust versus age, *Geophys. J. Int.*, **124**, 631–635, 1996.
- Hahn, A., H. Ahrendt, J. Meyer, and J.-H. Hufen, A model of magnetic sources within the Earth's crust compatible with the field measured by the satellite Magsat, *Geol. Jahrb., Reihe A*, **75**, 125–156, 1984.
- Hamilton, E. L., Shear-wave velocity versus depth in marine sediments: A review, *Geophysics*, **41**, 985–996, 1976.
- Hamilton, E. L., Sound velocity-density relations in sea-floor sediments and rocks, *J. Acoust. Soc. Am.*, **63**, 366–377, 1978.
- Hayes, D. E. (Ed.), *Marine Geological and Geophysical Atlas of the Circum-Antarctic to 30°S*, Antarct. Res. Ser., vol. 54, AGU, Washington, D. C., 1991.
- Heezen, B. C., R. P. Lynde Jr., and D. J. Fornari, Geological map of the Indian Ocean, in *Indian Ocean Geology and Biostratigraphy*, edited by J. R. Heirtzler et al., AGU, Washington, D. C., 1977.
- Holbrook, W. S., W. D. Mooney, and N. I. Christensen, The seismic velocity structure of the lower continental crust, in *The Lower Continental Crust*, edited by D. M. Fountain, R. Arculus, and R. Kay, pp. 1–43, Elsevier, New York, 1992.
- Holbrook, W. S., G. M. Purdy, R. E. Sheridan, L. Glover III, M. Talwani, J. Ewing, and D. Hutchinson, Seismic structure of the U.S. Mid-Atlantic continental margin, *J. Geophys. Res.*, **99**, 17,871–17,891, 1994.
- Inoue, H., Y. Fukao, K. Tanabe, and Y. Ogata, Whole mantle *P*-wave travel time tomography, *Phys. Earth Planet. Inter.*, **59**, 294–328, 1990.
- Jackson, H. R., and G. N. Oakey, Sedimentary thickness map of the Arctic Ocean, *The Geology of North America*, vol. L, *The Arctic Ocean*, edited by A. Grantz, L. Johnson, and J. F. Sweeney, Plate 5, Geol. Soc. of Am., Boulder, Colo., 1986.
- Jordan, T. H., Composition and development of the continental tectosphere, *Nature*, **274**, 544–548, 1978.
- Jordan, T. H., Continents as a chemical boundary layer, *Philos. Trans. R. Soc. London, Ser. A*, **301**, 359–373, 1981.
- Kovacs, A., J. S. Holladay, and C. J. Bergeron Jr., The footprint/altitude ratio for helicopter electromagnetic sounding of sea-ice thickness: Comparison of theoretical and field estimates, *Geophysics*, **60**, 374–380, 1995.
- Laske, G., and G. Masters, Constraints on global phase velocity maps by long-period polarization data, *J. Geophys. Res.*, **101**, 16,059–16,075, 1996.
- Le Pichon, X., J. Ewing, and R. E. Houtz, Deep-sea sediment velocity determination made while reflection profiling, *J. Geophys. Res.*, **73**, 2597–2613, 1968.
- Ludwig, W. J., and R. E. Houtz, Isopach map of sediments in the Pacific Ocean basin and marginal sea basins, Am. Assoc. of Pet. Geol., Tulsa, Okla., 1979.
- Ludwig, W. J., J. E. Nafe, and C. L. Drake, Seismic refraction, in *The Sea*, vol. 4, *Ideas and Observations on Progress in the Study of the Seas*, edited by A. E. Maxwell, pp. 53–84, Wiley-Interscience, New York, 1970.
- Masters, G., T. H. Jordan, P. G. Silver, and F. Gilbert, Aspherical Earth structure from fundamental spheroidal-mode data, *Nature*, **298**, 609–613, 1982.
- Masters, G., S. Johnson, G. Laske, and H. Bolton, A shear-velocity model of the mantle, *Philos. Trans. R. Soc. London A*, **354**, 1285–1411, 1996.
- Mechie, J., G. R. Keller, C. Prodehl, S. Gaciri, L. W. Braille, W. D. Mooney, D. Gajewski, and K. J. Sandmeier, Crustal structure beneath the Kenya Rift from axial profile data, *Tectonophysics*, **236**, 179–200, 1994.
- Meissner, R., *The Continental Crust: A Geophysical Approach*, 426 pp., Academic, San Diego, Calif., 1986.
- Montagner, J.-P., and T. Tanimoto, Global upper mantle tomography of seismic velocities and anisotropies, *J. Geophys. Res.*, **96**, 20,337–20,351, 1991.
- Mooney, W. D., Seismic methods for determining earthquake source parameters and lithospheric structure, in *Geophysical Framework of the Continental United States*, edited by L. C. Pakiser and W. D. Mooney, *Mem. Geol. Soc. Am.*, **172**, 11–34, 1989.
- Mooney, W. D., and L. W. Braille, The seismic structure of the continental crust and upper mantle of North America, in *The Geology of North America*, vol. A, *Overview*, edited by A. W. Bally and A. R. Palmer, pp. 39–52, Geol. Soc. of Am., Boulder, Colo., 1989.
- Mooney, W. D., and R. Meissner, Multi-genetic origin of crustal reflectivity: A review of seismic reflection profiling of the continental lower crust and Moho, in *The Continental Lower Crust*, edited by D. M. Fountain, R. Arculus, and R. Kay, pp. 39–52, Elsevier, New York, 1992.
- Nataf, H.-C., and Y. Ricard, 3SMAC: An a priori tomographic model of the upper mantle based on geophysical modeling, *Phys. Earth Planet. Inter.*, **95**, 101–122, 1996.

- National Geophysical Data Center, ETOPO-5, bathymetry/topography data, *Data Announc.* 88-MGG-02, Natl. Oceanic and Atmos. Admin., U.S. Dep. of Commer., Washington, D. C., 1988.
- Norris, A. W., Hudson Platform—Introduction, in *The Geology of North America*, vol. D-1, *Geology of Canada*, edited by D. F. Stott and J. D. Aitken, pp. 645–651, Geol. Soc. of Am., Boulder, Colo., 1993.
- Nur, A., and Z. Ben-Avraham, Oceanic plateaus, the fragmentation of continents, and mountain building, *J. Geophys. Res.*, *87*, 3644–3661, 1982.
- Orcutt, J. A., Structure of the Earth: Oceanic crust and uppermost mantle, *Rev. Geophys.*, *25*, 1177–1196, 1987.
- Pakiser, L. C., and W. D. Mooney (Eds.), *Geophysical Framework of the Continental United States*, *Mem. Geol. Soc. Am.*, *172*, 826 pp., 1989.
- Pavlenkova, N. I., Crustal and upper mantle structure in northern Eurasia from seismic data, *Adv. Geophys.*, *37*, 1–133, 1996.
- Phipps Morgan, J., W. J. Morgan, Y.-S. Zhang, and W. H. F. Smith, Observational hints for a plume-fed, suboceanic asthenosphere and its role in mantle convection, *J. Geophys. Res.*, *100*, 12,753–12,767, 1995.
- Prodehl, C., Structure of the Earth's crust and upper mantle, in *Encyclopedia of Geophysics*, vol. 11A, pp. 97–206, Landoldt Boernstein, Stuttgart, Germany, 1984.
- Pulliam, R. J., D. W. Vasco, and L. R. Johnson, Tomographic inversions for mantle *P* wave velocity structure based on the minimization of l^2 and l^1 norms of International Seismological Centre travel time residuals, *J. Geophys. Res.*, *98*, 699–734, 1993.
- Rabinowitz, P. D., N. Dipiazza, and P. K. Matthias, Sediment thickness map of the Indian Ocean, *Am. Assoc. of Pet. Geol.*, Tulsa, Okla., 1988.
- Raitt, R. W., The crustal rocks, in *The Sea*, vol. 3, *The Earth Beneath the Sea*, edited by M. N. Hill, pp. 85–102, Wiley-Interscience, New York, 1966.
- Renkin, M. L., and J. G. Sclater, Depth and age in the North Pacific, *J. Geophys. Res.*, *93*, 2919–2935, 1988.
- Ross, D. A., The Black Sea and the Sea of Azov, in *The Ocean Basins and Margins*, vol. 4a: *The Eastern Mediterranean*, edited by A. E. M. Nairs, W. H. Kanes, and F. G. Stehli, pp. 445–482, Plenum, New York, 1977.
- Salvador, A., Structure at the base and subcrop below Mesozoic marine section, Gulf of Mexico Basin, in *The Geology of North America*, vol. J, *The Gulf of Mexico Basin*, edited by A. Salvador, Geol. Soc. of Am., Boulder, Colo., 1986.
- Schubert, G., and D. Sandwell, Crustal volumes of the continents and of oceanic and continental submarine plateaus, *Earth Planet. Science Lett.*, *92*, 234–246, 1989.
- Shor, G. G., Jr., Seismic refraction profile in Coral Sea Basin, *Science*, *158*, 911–913, 1967.
- Shor, G. G., Jr., H. K. Kirk, and H. W. Menard, Crustal structure of the Melanesian area, *J. Geophys. Res.*, *76*, 2562–2586, 1971.
- Smith, M. F., Imaging the Earth's aspherical structure with free oscillation frequency and attenuation measurements, Ph.D. thesis, 97 pp., Univ. of Calif., San Diego, La Jolla, 1989.
- Soller, D. R., R. D. Ray, and R. D. Brown, A new global crustal thickness model, *Tectonics*, *1*, 125–149, 1982.
- Spudich, P., and J. Orcutt, Petrology and porosity of an oceanic crustal site: Results from wave form modeling of seismic refraction data, *J. Geophys. Res.*, *85*, 1409–1433, 1980.
- Tanimoto, T., Crustal structure of the Earth, *Global Earth Physics: A Handbook of Physical Constants*, *AGU Ref. Shelf*, vol. 1, edited by T. J. Ahrens, pp. 214–224, AGU, Washington, D. C., 1995.
- Trampert, J., and J. H. Woodhouse, Global phase velocity maps of Love and Rayleigh waves between 40 and 150 seconds, *Geophys. J. Int.*, *122*, 675–690, 1995.
- Tucholke, B. E., Structure of basement and distribution of sediments in the western North Atlantic Ocean, in *The Geology of North America*, vol. M, *The Western North Atlantic Region*, edited by P. R. Vogt and B. E. Tucholke, pp. 331–340, Geol. Soc. of Am., Boulder, Colo., 1986.
- Tucholke, B. E., and E. Uchupi, Thickness of sedimentary cover, in *International Geology-Geophysical Atlas of the Atlantic Ocean*, edited by G. B. Udintsev, sheet 1, Russ. Minist. of Geol., Russ. Acad. of Sci., Moscow, 1989a.
- Tucholke, B. E., and E. Uchupi, Thickness of sedimentary cover, in *International Geology-Geophysical Atlas of the Atlantic Ocean*, edited by G. B. Udintsev, sheet 2, Russ. Minist. of Geol., Russ. Acad. of Sci., Moscow, 1989b.
- Vasco, D. W., L. R. Johnson, and J. Pulliam, Lateral variations in mantle velocity structure and discontinuities determined from *P*, *PP*, *S*, *SS*, and *SS-S_dS* travel times residuals, *J. Geophys. Res.*, *100*, 24,037–24,059, 1995.
- Voggenreiter, W., H. Hoetzel, and J. Mechie, Low-angle detachment origin for the Red Sea rift system?, *Tectonophysics*, *150*, 51–75, 1988.
- Weidick, A., C. E. Boggild, and N. T. Knudsen, Glacier inventory and atlas of West Greenland, *Rapp.* *158*, 193 pp., Gronlands Geol. Undersogelse, Copenhagen, 1992.
- White, R. S., D. McKenzie, and R. K. O'Nions, Oceanic crustal thickness from seismic measurements and rare earth element inversions, *J. Geophys. Res.*, *97*, 19,683–19,715, 1992.
- Woodhouse, J. H., and A. M. Dziewonski, Mapping of the upper mantle: Three-dimensional modeling of Earth structure by inversion of seismic waveforms, *J. Geophys. Res.*, *89*, 5953–5986, 1984.
- Woodward, R. L., and G. Masters, Global upper mantle structure from long-period differential travel times, *J. Geophys. Res.*, *96*, 6351–6377, 1991.
- Zielhuis, A., and G. Nolet, Shear-wave velocity variations in the upper mantle beneath central Europe, *Geophys. J. Int.*, *117*, 695–715, 1994.

G. Laske and T. G. Masters, IGPP, Scripps Institution of Oceanography, University of California, San Diego, La Jolla, CA 92093-0225. (e-mail: glaske@ucsd.edu; gmasters@ucsd.edu)

W. D. Mooney, U.S. Geological Survey, 345 Middlefield Road, MS 977, Menlo Park, CA 94025. (e-mail: mooney@andreas.wr.usgs.gov)

(Received November 12, 1996; revised July 2, 1997; accepted July 24, 1997.)